

Chapter 2

The Standard ASW Method

Our survey of the ASW method starts with an outline of the standard scheme, which, within the framework of density functional theory and the local density approximation, allows for both fast and conceptually simple calculations of the ground state properties of solids. The standard ASW method was originally developed by Williams, Kübler and Gelatt [78]. For excellent presentations of the method the reader is referred to both the original work and a number of reviews, which also shaped the form of the present chapter [23, 27, 32, 45, 53, 73]. A first impression of selected applications can be gained from Refs. [23, 25–27, 45, 51, 65].

After defining the ASW basis set we will construct the elements of the secular matrix. Via the variational principle the latter allows to numerically determine the expansion coefficients of the ground state wave function as expanded in terms of the basis functions. Knowledge of the wave function enables for calculation of the electron density and the effective single-particle potential, the latter of which closes the self-consistency cycle. Finally, we sketch the calculation of the total energy. The standard ASW method forms the basis for the much more involved full-potential methods to be described in Chaps. 4 and 5. For this reason the presentation will be both simple and comprehensive.

2.1 Setup of Basis Functions

The goal of any first-principles method is to determine the single-particle wave function from Schrödinger's equation

$$[-\Delta + v_\sigma(\mathbf{r}) - \varepsilon]\psi_\sigma(\varepsilon, \mathbf{r}) = 0, \quad (2.1.1)$$

where, as usual, $-\Delta$, the negative of the Laplacian, designates the operator of the kinetic energy. $\psi_\sigma(\varepsilon, \mathbf{r})$ is a spinor component of the wave function and σ labels the spin index. In addition, $v_\sigma(\mathbf{r})$ denotes the spin-dependent, effective single-particle potential. It may be provided by density functional theory, in which case (2.1.1) is just the Kohn-Sham equation. As a matter of fact, solving Schrödinger's equation

Fig. 2.1 Muffin-tin

in the general form (2.1.1) is usually far from straightforward. However, within density functional theory we are aiming at the ground state and may thus employ the variational principle. Hence, we expand the wave function in a set of basis functions and seek the stationary states by varying the expansion coefficients and possibly the shape of the basis functions themselves. Since in practice we are forced to use a finite and, hence, incomplete set of functions, the choice of basis functions is very important as concerns both the quality of the final solution and the numerical effort to find it. As already mentioned in the introduction, it is this selection of a basis set, which distinguishes the different methods nowadays used for electronic structure calculations. The ASW method belongs to the partial-wave methods and is based on Slater's muffin-tin approximation. In addition, it uses spherical waves as well as Andersen's linearization.

Obviously, the basis functions themselves should at best also fulfill Schrödinger's equation (2.1.1). Yet, this would again lead to the above mentioned difficulties and concessions are thus necessary. A very popular one is based on Slater's observation that the crystal potential, while being dominated by the purely atomic and, hence, spherical symmetric contributions near the nuclei, is rather flat in the regions far away from the atomic centers [70]. Idealizing this situation, Slater proposed the muffin-tin approximation (MTA), which adopts the geometry of a muffin-tin as visualized in Fig. 2.1. To be specific, the MTA replaces the full crystal potential by its spherical symmetric average within the non-overlapping muffin-tin spheres and a constant value, the so-called muffin-tin zero v_{MTZ} , in the remaining interstitial region. The effective single-particle potential is thus modeled as

$$\begin{aligned} v_{\sigma}^{MT}(\mathbf{r}) &= v_{MTZ} \Theta_I + \sum_{\mu i} v_{i\sigma}^{MT}(\mathbf{r}_{\mu i}) \Theta_{\mu i} \\ &= v_{MTZ} + \sum_{\mu i} \hat{v}_{i\sigma}^{MT}(\mathbf{r}_{\mu i}). \end{aligned} \quad (2.1.2)$$

Here we have defined

$$\mathbf{r}_{\mu i} := \mathbf{r} - \mathbf{R}_{\mu i} \quad \text{and} \quad \mathbf{R}_{\mu i} := \mathbf{R}_{\mu} + \boldsymbol{\tau}_i, \quad (2.1.3)$$

where \mathbf{R}_μ is a lattice vector and $\boldsymbol{\tau}_i$ the position of the nucleus labeled i in the unit cell; σ again denotes the spin index. The step functions Θ_I and $\Theta_{\mu i}$ limit the range of the functions, which are attached to them, to the interstitial region and the muffin-tin sphere of radius s_i centered at site $\mathbf{R}_{\mu i}$, respectively. In the second line of (2.1.2) we have added an alternative notation using the potential

$$\hat{v}_{i\sigma}^{MT}(\mathbf{r}_{\mu i}) := [v_{i\sigma}^{MT}(\mathbf{r}_{\mu i}) - v_{MTZ}] \Theta_{\mu i}. \quad (2.1.4)$$

It just represents a constant shift of all potentials inside the atomic spheres but may be likewise interpreted as a splitting of the total potential into two parts, one of which extends through all space and is rather flat (or constant, as in the present case). Below, we will denote this contribution as the pseudo part, since inside the muffin-tin spheres it has no meaning in itself. In contrast, the remaining local parts contain all the intraatomic details of the potential but are confined to the respective muffin-tin spheres. The total potential is then arrived at by adding, inside the spheres, the local contributions to the pseudo part.

Within the MTA the choice of the sphere radii is restricted by the plausible requirement that the spheres must not overlap. A somewhat different point of view is taken by the atomic-sphere approximation (ASA) invented by Andersen [4, 5], which requires the sum of the atomic sphere volumes to equal the cell volume,

$$\sum_i \tilde{\Omega}_i := \sum_i \frac{4\pi}{3} S_i^3 \stackrel{!}{=} \Omega_c. \quad (2.1.5)$$

Here $\tilde{\Omega}_i$ and Ω_c denote the volumes of the atomic sphere i and the unit cell, respectively, while S_i is the radius of the atomic sphere. In general, we will use a tilde for quantities connected to the space-filling atomic spheres. As it stands, the ASA leads to a formal elimination of the interstitial region. This serves the purpose of minimizing the errors coming with the muffin-tin approximation as well as with the linearization to be described below, which both are largest for the interstitial region. Furthermore, it has been demonstrated that for moderate overlaps of the spheres the ASA provides a better prescription of the potential in the bonding region between the atoms and thus mimics the full potential in a better way than the MTA does [7]. In the following, we will opt for the ASA but still want to keep things on general grounds as long as possible. Thus, we formally stay with the muffin-tin form (2.1.2) of the potential without explicitly making use of the atomic-sphere approximation.

Having modeled the effective single-particle potential in the way just described we will next construct the basis functions from the muffin-tin potential. This is done by first solving Schrödinger's equation separately in the atomic spheres as well as in the interstitial region and then matching the resulting partial waves continuously and differentially at the sphere boundaries. This will lead to a single basis function, an *augmented spherical wave*. To be specific, the basis functions have to obey Schrödinger's equation (2.1.1) with the potential replaced by the muffin-tin potential (2.1.2),

$$\begin{aligned} & [-\Delta + v_\sigma^{MT}(\mathbf{r}) - \varepsilon] \varphi_\sigma(\varepsilon, \mathbf{r}) \\ & = [-\Delta + v_\sigma^{MT}(\mathbf{r}) - v_{MTZ} - \kappa^2] \varphi_\sigma(\varepsilon, \mathbf{r}) = 0, \end{aligned} \quad (2.1.6)$$

separately in the interstitial region and the atomic spheres. Here, we have in the second step referred the potential to the muffin-tin zero and defined

$$\kappa^2 = \varepsilon - v_{MTZ}. \quad (2.1.7)$$

By construction, the basis functions are only approximate solutions of the correct Schrödinger equation (2.1.1), where the potential was still unrestricted. This is a consistent approximation within the standard ASW method, which uses the atomic-sphere approximation throughout. But even for a full-potential method use of the ASA for the construction of the basis functions is justified by the fact that the basis functions enter only as part of the wave function and inaccuracies of the former are cured by the variational determination of the latter. Use of the MTA (or ASA) for the construction of the basis functions may thus be regarded as an optimal balance between effort and accuracy.

Starting the setup of the partial waves in the interstitial region we combine (2.1.2) and (2.1.6) and arrive at Helmholtz's equation

$$[-\Delta - \kappa^2]\varphi_\sigma(\kappa^2, \mathbf{r}) = 0. \quad (2.1.8)$$

As well known, this differential equation is trivially solved by plane waves. However, we may likewise choose spherical waves, which are centered at the atomic sites and consist of products of spherical harmonics and radial functions. The latter are solutions of the free-particle radial Schrödinger equation for energy κ^2 and, hence, well known as spherical Bessel, Neumann or Hankel functions. Note that the singularities of the latter two functions are located at the respective origins, i.e. at the centers of the atomic spheres and thus do not spoil the analytic behavior of these functions in the interstitial region.

The choice of spherical waves is common to the Korringa-Kohn-Rostoker (KKR) [40, 43], linear muffin-tin orbitals (LMTO) [5], and ASW methods. In particular, the KKR method opts for spherical Neumann functions for the radial part. The interstitial part of the basis function reads as

$$N_{L\kappa\sigma}^\infty(\mathbf{r}_{\mu i})\Theta_I := N_{L\kappa}^I(\mathbf{r}_{\mu i}) := N_{L\kappa}(\mathbf{r}_{\mu i})\Theta_I, \quad (2.1.9)$$

where

$$N_{L\kappa}(\mathbf{r}_{\mu i}) := -\kappa^{l+1}n_l(\kappa r_{\mu i})Y_L(\hat{\mathbf{r}}_{\mu i}). \quad (2.1.10)$$

Here, $n_l(\kappa r_{\mu i})$ denotes the spherical Neumann function in the notation of Abramowitz and Stegun [1, Chap. 10]. The index $L = (l, m)$ is a compose of the angular momentum and the magnetic quantum numbers. $Y_L(\hat{\mathbf{r}}_{\mu i})$ denotes a spherical harmonic or rather a cubic harmonic in the form proposed in Sect. 7.2 and $\hat{\mathbf{r}}_{\mu i}$ stands for a unit vector. The prefactor κ^{l+1} serves the purpose of canceling the leading κ -dimension of the spherical Neumann function and making the radial part of the function $N_{L\kappa}(\mathbf{r}_{\mu i})$ a real function, hence, easy to deal with in computer implementations. In passing, we mention that, in the context of the ASW method, the latter function is commonly also designated as the Neumann function.

Of course, we could likewise opt for spherical Hankel functions as the radial part of the basis functions. In this case the interstitial part of the basis function would have assumed the form

$$H_{L\kappa\sigma}^{\infty}(\mathbf{r}_{\mu i})\Theta_I := H_{L\kappa}^I(\mathbf{r}_{\mu i}) := H_{L\kappa}(\mathbf{r}_{\mu i})\Theta_I \quad (2.1.11)$$

with

$$H_{L\kappa}(\mathbf{r}_{\mu i}) := i\kappa^{l+1}h_l^{(1)}(\kappa r_{\mu i})Y_L(\hat{\mathbf{r}}_{\mu i}), \quad (2.1.12)$$

where $h_l^{(1)}(\kappa r_{\mu i})$ is the spherical Hankel function in the notation of Abramowitz and Stegun and, as before, the function $H_{L\kappa}(\mathbf{r}_{\mu i})$ is also named a Hankel function. Again, the prefactor serves the purpose of canceling the leading κ -dimension and making the radial part a real function. Yet, the latter is true for negative energies κ^2 only, where, however, the spherical Hankel functions offer the additional great advantage of decaying exponentially in space. This is an appealing behavior especially if non-crystalline or finite systems are dealt with. Nevertheless, the fact that the radial part in general is a complex function makes the Hankel functions rather unsuitable for the KKR method.

As was first pointed out by Andersen at the beginning of the 1970's the energy (κ -) dependence of the final basis function turns out to be rather weak. This observation led Andersen to argue that it is sufficient to retain only the first two terms of the corresponding Taylor series [3, 69]. Formally suppressing the interstitial region by introducing the atomic-sphere approximation, Andersen was able to remove even the linear term for the interstitial functions and to arrive at energy-independent functions with a fixed value of κ^2 for the radial part. Of course, this value was expected to be in the region of interest, i.e. between -1 Ryd and $+1$ Ryd. With energy-independent basis functions at hand it was possible to replace the time consuming root tracing needed in the KKR method for calculating the single-particle energies by a simple eigenvalue problem. This meant a tremendous cut down of computing times since the eigenvalue problem is by at least an order of magnitude faster to solve. Andersen's work thus marked the starting point for a number of new, the so-called linear methods among them the linear muffin-tin orbitals (LMTO) method, the linear augmented plane wave (LAPW) method, and the ASW method, which in the sense just mentioned are superior to the classical schemes such as the augmented plane wave (APW) method and the Korringa-Kohn-Rostoker (KKR) method [5, 6, 8, 45, 69]. The albeit small limitations due to the energy linearization could be cured by employing so-called multiple- κ sets, which use basis functions with two or three different values of the interstitial energy κ^2 . However, for the standard LMTO and ASW methods, which use the atomic-sphere approximation, the effect is almost negligible and multiple- κ sets are thus not used. Yet, they will be needed in those full-potential methods, which use the muffin-tin approximation, hence, a finite interstitial region. In order to prepare for later developments we include the energy parameter κ already in the present notation.

With the energy parameter κ fixed, a greater flexibility for the choice of basis functions is obtained since there is no longer the need to use a single type of function for the whole energy range. In contrast, we are by now able to opt for that type

of function, which offers the best properties and then fix the energy parameter κ^2 to a suitable value within the above proposed range of -1 Ryd and $+1$ Ryd. To be specific, in the ASW method we set $\kappa^2 = -0.015$ Ryd and opt for the Hankel function $H_{L\kappa\sigma}^\infty(\mathbf{r}_{\mu i})$, which for this energy offers the above mentioned advantages of being real and decaying exponentially. Nevertheless, we could have likewise chosen a positive energy parameter, in which case the ASW method uses the Neumann function $N_{L\kappa\sigma}^\infty(\mathbf{r}_{\mu i})$ as the interstitial part of the basis function. In passing, we mention that the LMTO method uses $\kappa^2 = 0$ Ryd, in which case both types of functions are identical and assume a particularly simple form as will be discussed in Chap. 3 [5].

While staying with the negative energy case and, hence, using the Hankel function (2.1.11) as the interstitial part of the basis function we will not utilize the simplifications offered by the asymptotic decay of the spherical Hankel functions for negative energies but rather stay with a more general derivation. This will save us an extra discussion for the Neumann functions. In practice, this means that all the derivations formulated below with Hankel functions will also hold for Neumann functions. Note that, in contrast to previous definitions of the ASW basis functions [78], the functions (2.1.10) and (2.1.12) do not contain an extra i^l -factor this making them (as well as the real-space structure constants to be defined later on) real quantities in the respective energy range. In addition, our new choice leads to considerable numerical simplifications for the full-potential ASW methods to be derived in Chaps. 4 and 5.

Having discussed the interstitial basis functions we next turn to the regions inside the atomic spheres. Here, the potential shows all the intraatomic details and, hence, solving Schrödinger's equation is more complicated. However, within the muffin-tin approximation the full crystal potential is reduced to its spherical symmetric average inside the atomic spheres this allowing for a separation of Schrödinger's equation into angular and radial parts. While the former again leads to spherical harmonics the latter can be determined numerically subject to the conditions of continuous and differentiable matching to the interstitial basis function. As a consequence, in addition to being used in the interstitial region only, the interstitial basis functions serve the purpose of providing boundary conditions for the solution of Schrödinger's equation inside the spheres. In the atomic-sphere approximation, due to the formal elimination of the interstitial region, it is the second aspect alone, which survives. For this reason, the interstitial basis functions are also called envelope functions. We will discuss especially the mathematical aspects of the envelope functions in more detail in Chap. 3.

Turning to the region inside the spheres, we first concentrate on that single atomic sphere where the spherical wave is centered. In this so-called on-center sphere spherical symmetry is obvious and we readily arrive at the intraatomic basis function, which is called the augmented Hankel function,

$$H_{L\kappa\sigma}^\infty(\mathbf{r}_{\mu i})\Theta_{\mu i} := \tilde{H}_{L\kappa\sigma}(\mathbf{r}_{\mu i}) := \tilde{h}_{l\kappa\sigma}(r_{\mu i})Y_L(\hat{\mathbf{r}}_{\mu i})\Theta_{\mu i}. \quad (2.1.13)$$

Its radial part obeys the radial Schrödinger equation

$$\begin{aligned}
& \left[-\frac{1}{r_{\mu i}} \frac{\partial^2}{\partial r_{\mu i}^2} r_{\mu i} + \frac{l(l+1)}{r_{\mu i}^2} + v_{i\sigma}^{MT}(r_{\mu i}) - v_{MTZ} - E_{l\kappa i\sigma}^{(H)} \right] \tilde{h}_{l\kappa\sigma}(r_{\mu i}) \\
& = \left[-\frac{1}{r_{\mu i}} \frac{\partial^2}{\partial r_{\mu i}^2} r_{\mu i} + \frac{l(l+1)}{r_{\mu i}^2} + \hat{v}_{i\sigma}^{MT}(r_{\mu i}) - E_{l\kappa i\sigma}^{(H)} \right] \tilde{h}_{l\kappa\sigma}(r_{\mu i}) = 0.
\end{aligned} \tag{2.1.14}$$

The numerical solution of this equation as well as the determination of the Hankel energy $E_{l\kappa i\sigma}^{(H)}$ are subject to three boundary conditions, namely, the regularity of the radial function $\tilde{h}_{l\kappa\sigma}(r_{\mu i})$ at its origin and the continuous and differentiable matching at the sphere boundary,

$$\left[\left(\frac{\partial}{\partial r_{\mu i}} \right)^n (\tilde{h}_{l\kappa\sigma}(r_{\mu i}) - i\kappa^{l+1} h_l^{(1)}(\kappa r_{\mu i})) \right]_{r_{\mu i}=s_i} = 0, \quad n = 0, 1. \tag{2.1.15}$$

Still, in order to solve (2.1.14) numerically, we have to specify the principal quantum numbers and the angular momenta l of all states to be taken into account. For the angular momenta we include all l values ranging from 0 to some maximum value l_{low} . Usually, the latter is set to 2 or 3 depending on the respective atom. While for main group elements we include s and p states, we account also for d and possibly f orbitals in case of transition metal and rare earth atoms. All these states form the ASW basis set, which, following Andersen, we call the set of lower waves.

The principal quantum number of each partial wave, which corresponds to the number of nodes once the angular momentum of a lower wave has been fixed, is selected in accordance with the outer electrons of each atom. To be specific, we first divide all states of an atom into core and valence states. The former are characterized by vanishing value and slope at the sphere boundary and, hence, confined to the inner region of the atomic sphere. As a consequence, while contributing to the electron density the core states are not included in the ASW basis set, which comprises only the valence states. We will come back to the core states at the end of this section. In general, only the outermost state for each atom and $l \leq l_{low}$ is chosen as a valence state and included in the basis set. This is done implicitly and the respective principal quantum number thus suppressed from the notation. Of course, there might be situations, where, in addition to the outermost valence states, high lying core states should also be included in the ASW basis set. However, in order to take the notation simple, we will not deal with such cases in the present context.

By now we have augmented the spherical wave centered at $\mathbf{R}_{\mu i}$ inside its on-center sphere. In all other atomic spheres of the crystal, which are centered at sites $\mathbf{R}_{vj} \neq \mathbf{R}_{\mu i}$, and referred to as the off-center spheres, augmentation is not as straightforward. This is due to the fact that the envelope function centered at $\mathbf{R}_{\mu i}$ lacks spherical symmetry relative to the centers \mathbf{R}_{vj} of the off-center spheres. Yet, the problem can be resolved by applying the expansion theorem for the envelope functions, which allows to expand the Hankel function centered at $\mathbf{R}_{\mu i}$ as defined by (2.1.12) in Bessel functions centered at \mathbf{R}_{vj} ,

$$H_{L\kappa}(\mathbf{r}_{\mu i}) = \sum_{L'} J_{L'\kappa}(\mathbf{r}_{vj}) B_{L'L\kappa}(\mathbf{R}_{vj} - \mathbf{R}_{\mu i}). \tag{2.1.16}$$

The expansion theorem is valid for all vectors \mathbf{r} , which fulfill the condition $|\mathbf{r}_{vj}| < |\mathbf{R}_{vj} - \mathbf{R}_{\mu i}|$, thus for all \mathbf{r} lying within a sphere of radius equal to the distance between the two centers and centered at \mathbf{R}_{vj} . However, we point out that the L' -sum in (2.1.16) in general does not converge and thus needs special care. We will come back to this issue later on. The Bessel function

$$J_{L'\kappa}(\mathbf{r}_{vj}) := \kappa^{-l'} j_{l'}(\kappa r_{vj}) Y_{L'}(\hat{\mathbf{r}}_{vj}) \quad (2.1.17)$$

like the Hankel function given by (2.1.12), arises from solving Helmholtz' equation (2.1.8). $j_{l'}(\kappa r_{vj})$ denotes a spherical Bessel function. The prefactor again was introduced to cancel the leading κ -dimension and to make the radial part a real quantity for any value of κ^2 .

The expansion coefficients entering (2.1.16) are the structure constants known from the KKR method [33, 66]. Their calculation as well as the proof of the expansion theorem will be given in full detail in Sects. 3.6 and 3.7. Here we present the result

$$B_{L'L\kappa}(\mathbf{R}_{vj} - \mathbf{R}_{\mu i}) = 4\pi \sum_{L''} i^{l-l'-l''} \kappa^{l+l'-l''} c_{LL'L''} H_{L''\kappa}(\mathbf{R}_{vj} - \mathbf{R}_{\mu i}), \quad (2.1.18)$$

which is valid for $\mathbf{R}_{vj} \neq \mathbf{R}_{\mu i}$ and where

$$c_{LL'L''} = \int d^2\hat{\mathbf{r}} Y_L^*(\hat{\mathbf{r}}) Y_{L'}(\hat{\mathbf{r}}) Y_{L''}(\hat{\mathbf{r}}) \quad (2.1.19)$$

denotes a (real) Gaunt coefficient.

With the expansion theorem (2.1.16) at hand we are ready to augment the spherical wave in any of the off-center spheres. This is due to the fact that the Bessel functions given by (2.1.17) are centered at the center of this sphere and thus reflect the spherical symmetry relative to the respective atomic site. As a consequence, the basis function in the off-center sphere centered at \mathbf{R}_{vj} can be expressed in terms of augmented Bessel functions

$$\tilde{J}_{L'\kappa\sigma}(\mathbf{r}_{vj}) := \tilde{j}_{l'\kappa\sigma}(r_{vj}) Y_{L'}(\hat{\mathbf{r}}_{vj}) \Theta_{vj}. \quad (2.1.20)$$

Their radial parts obey the radial Schrödinger equation

$$\begin{aligned} & \left[-\frac{1}{r_{vj}} \frac{\partial^2}{\partial r_{vj}^2} r_{vj} + \frac{l'(l'+1)}{r_{vj}^2} + v_{j\sigma}^{MT}(r_{vj}) - v_{MTZ} - E_{l'\kappa j\sigma}^{(J)} \right] \tilde{j}_{l'\kappa\sigma}(r_{vj}) \\ &= \left[-\frac{1}{r_{vj}} \frac{\partial^2}{\partial r_{vj}^2} r_{vj} + \frac{l'(l'+1)}{r_{vj}^2} + \hat{v}_{j\sigma}^{MT}(r_{vj}) - E_{l'\kappa j\sigma}^{(J)} \right] \tilde{j}_{l'\kappa\sigma}(r_{vj}) = 0. \end{aligned} \quad (2.1.21)$$

As for the augmented Hankel function, the numerical solution of this differential equation as well as the determination of the Bessel energy $E_{l'\kappa j\sigma}^{(J)}$ are subject to the conditions of continuous and differentiable matching at the sphere boundary,

$$\left[\left(\frac{\partial}{\partial r_{vj}} \right)^n (\tilde{j}_{l'\kappa\sigma}(r_{vj}) - \kappa^{-l'} j_{l'}(\kappa r_{vj})) \right]_{r_{vj}=s_j} = 0, \quad n = 0, 1, \quad (2.1.22)$$

as well as the regularity of the radial function $\tilde{J}'_{l'\kappa\sigma}(r_{vj})$ at the origin. Note that the radial equations (2.1.14) and (2.1.21) are identical and, hence, the difference between the augmented functions $\tilde{h}_{l\kappa\sigma}$ and $\tilde{J}_{l\kappa\sigma}$ as well as the energies $E_{l\kappa i\sigma}^{(H)}$ and $E_{l\kappa i\sigma}^{(J)}$ results alone from the different boundary conditions (2.1.15) and (2.1.22).

With the radial part at hand we arrive at the following expression for the basis function centered at $\mathbf{R}_{\mu i}$ inside the off-center sphere centered at \mathbf{R}_{vj}

$$H_{L\kappa\sigma}^{\infty}(\mathbf{r}_{\mu i})\Theta_{vj} = \sum_{L'} \tilde{J}_{L'\kappa\sigma}(\mathbf{r}_{vj}) B_{L'L\kappa}(\mathbf{R}_{vj} - \mathbf{R}_{\mu i}). \quad (2.1.23)$$

Note that, due to the identity of $H_{L\kappa}$ and $\tilde{H}_{L\kappa\sigma}$ as well as $J_{L\kappa}$ and $\tilde{J}_{L\kappa\sigma}$ at the sphere boundary, the expansion coefficients in (2.1.16) and (2.1.23) are the same. In passing, we mention that (2.1.16) and (2.1.23) are also called the one-center expansion of the Hankel envelope function and the basis function in terms of Bessel envelope functions and augmented Bessel functions, respectively. To be more detailed, they constitute the one-center expansions in the off-center spheres. In contrast, the one-center expansion of a Hankel envelope function and an augmented Hankel function, respectively, in their on-center sphere are just these functions themselves.

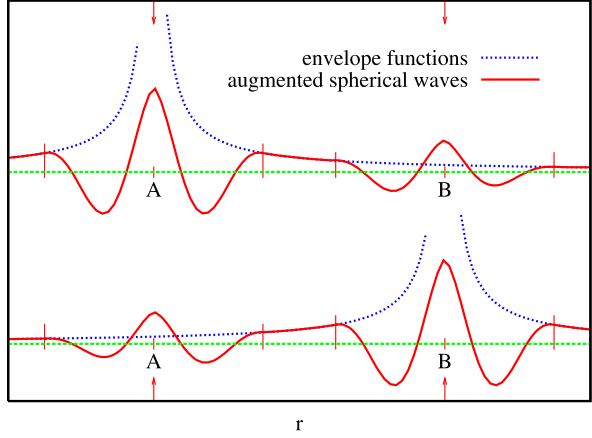
As for the augmented Hankel functions we still need to specify the maximum angular momentum as well as the principal quantum numbers to be used for solving (2.1.21). As already mentioned, the one-center expansion in the off-center spheres, i.e. the expression of the Hankel function in terms of an angular momentum series over Bessel functions via the expansions (2.1.16) and (2.1.23) does not converge. For that reason, we would in principle have to include infinitely many Bessel functions. However, as we will see in the subsequent section, we will be able, by combining two such series expansions, to end up with only few terms in the series. We denote the corresponding angular momentum cutoff as l_{int} , which is usually chosen as $l_{int} = l_{low} + 1$. Again following Andersen, we call the partial waves with $l_{low} < l \leq l_{int}$ intermediate waves. In contrast, partial waves with $l > l_{int}$ are named higher waves. The principal quantum number required for solving (2.1.21) is chosen in accordance with the valence states for the corresponding atom just in the same manner as for the augmented Hankel function above.

Finally, combining (2.1.11), (2.1.13), and (2.1.23), we construct the full basis function, the *augmented spherical wave*

$$H_{L\kappa\sigma}^{\infty}(\mathbf{r}_{\mu i}) = H_{L\kappa}^I(\mathbf{r}_{\mu i}) + \tilde{H}_{L\kappa\sigma}(\mathbf{r}_{\mu i}) + \sum_{L'vj} (1 - \delta_{\mu\nu}\delta_{ij}) \tilde{J}_{L'\kappa\sigma}(\mathbf{r}_{vj}) B_{L'L\kappa}(\mathbf{R}_{vj} - \mathbf{R}_{\mu i}), \quad (2.1.24)$$

which is completely specified by its center, $\mathbf{R}_{\mu i}$, the composite angular momentum index $L = (l, m)$, and the spin index σ ; note that the energy κ^2 is kept only as a parameter. In addition, the augmented spherical wave is continuous and differentiable in all space. This is illustrated in Fig. 2.2, where we display two augmented spherical waves centered at two different sites. We can easily identify the envelope functions by the singularity at their respective origins. Inside the on-center spheres (labeled “A” and “B” in the upper and lower curve, respectively) as well as the

Fig. 2.2 Augmented spherical waves centered at different sites, labeled “A” and “B”



off-center spheres (labeled “B” and “A” in the upper and lower curve, respectively) these envelope functions are replaced by the augmented functions. This construction then gives rise to the augmented spherical waves, which have the above mentioned properties.

Since the ASW basis functions arise from solutions of Schrödinger’s equation in the respective portions of space, each of these functions is quite well adapted to the actual problem and only a relatively small number of basis functions is needed for the expansion of the final wave function; as already mentioned above, typically 9 states (s, p, d) per atom are sufficient and for atoms with f electrons we end up with 16 states. Such a compact basis set is usually called a minimal basis set. As an additional bonus, the ASW basis functions, being closely related to atomic-like functions, allow for a natural interpretation of the calculated results.

In a final step, we take into account crystal translational symmetry and use Bloch sums of the basis functions defined as

$$D_{L\kappa\sigma}^{\infty}(\mathbf{r}_i, \mathbf{k}) := \sum_{\mu} e^{i\mathbf{k}\mathbf{R}_{\mu}} H_{L\kappa\sigma}^{\infty}(\mathbf{r}_{\mu i}), \quad (2.1.25)$$

where

$$\mathbf{r}_i = \mathbf{r} - \boldsymbol{\tau}_i \quad (2.1.26)$$

and the symbol D is convention. Note that we will refer to both the functions (2.1.24) and (2.1.25) as basis functions but the actual meaning will be always clear from the context.

In order to prepare for forthcoming sections we define, in addition, the Bloch sum of the envelope function (2.1.11) by

$$D_{L\kappa}(\mathbf{r}_i, \mathbf{k}) := \sum_{\mu} (1 - \delta_{\mu 0} \delta(\mathbf{r}_i)) e^{i\mathbf{k}\mathbf{R}_{\mu}} H_{L\kappa}(\mathbf{r}_{\mu i}). \quad (2.1.27)$$

In complete analogy to (2.1.11) its interstitial part reads as

$$D_{L\kappa}^I(\mathbf{r}_i, \mathbf{k}) := \sum_{\mu} e^{i\mathbf{k}\mathbf{R}_{\mu}} H_{L\kappa}^I(\mathbf{r}_{\mu i}) = D_{L\kappa}(\mathbf{r}_i, \mathbf{k}) \Theta_I. \quad (2.1.28)$$

Moreover, we define the Bloch-summed structure constants as

$$\begin{aligned} B_{L'L\kappa}(\boldsymbol{\tau}_j - \boldsymbol{\tau}_i, \mathbf{k}) &:= \sum_{\mu} (1 - \delta_{\mu\nu} \delta_{ij}) e^{i\mathbf{k}\mathbf{R}_{\mu}} B_{L'L\kappa}(\boldsymbol{\tau}_j - \boldsymbol{\tau}_i - \mathbf{R}_{\mu}) \\ &= 4\pi \sum_{L''} i^{l-l'-l''} \kappa^{l+l'-l''} c_{LL'L''} D_{L''\kappa}(\boldsymbol{\tau}_j - \boldsymbol{\tau}_i, \mathbf{k}), \end{aligned} \quad (2.1.29)$$

where we have used the identities (2.1.18) and (2.1.27) in the second step. Hence, we get for the Bloch-summed basis function the result

$$\begin{aligned} D_{L\kappa\sigma}^{\infty}(\mathbf{r}_i, \mathbf{k}) &= D_{L\kappa}^I(\mathbf{r}_i, \mathbf{k}) + \tilde{H}_{L\kappa\sigma}(\mathbf{r}_i) \\ &\quad + \sum_{L'j} \tilde{J}_{L'\kappa\sigma}(\mathbf{r}_j) B_{L'L\kappa}(\boldsymbol{\tau}_j - \boldsymbol{\tau}_i, \mathbf{k}). \end{aligned} \quad (2.1.30)$$

Finally, combining the previous identities we write the wave function entering the variational procedure as a linear combination of the just defined Bloch sums

$$\begin{aligned} \psi_{\mathbf{k}\sigma}(\mathbf{r}) &= \sum_{L\kappa i} c_{L\kappa i\sigma}(\mathbf{k}) D_{L\kappa\sigma}^{\infty}(\mathbf{r}_i, \mathbf{k}) \\ &= \sum_{L\kappa i} c_{L\kappa i\sigma}(\mathbf{k}) D_{L\kappa}^I(\mathbf{r}_i, \mathbf{k}) \\ &\quad + \sum_{L\kappa i} c_{L\kappa i\sigma}(\mathbf{k}) \tilde{H}_{L\kappa\sigma}(\mathbf{r}_i) \\ &\quad + \sum_{L'\kappa j} a_{L'\kappa j\sigma}(\mathbf{k}) \tilde{J}_{L'\kappa\sigma}(\mathbf{r}_j), \end{aligned} \quad (2.1.31)$$

where, in the second step, we have used the representation (2.1.30) as well as the abbreviation

$$a_{L'\kappa j\sigma}(\mathbf{k}) = \sum_{Li} c_{L\kappa i\sigma}(\mathbf{k}) B_{L'L\kappa}(\boldsymbol{\tau}_j - \boldsymbol{\tau}_i, \mathbf{k}). \quad (2.1.32)$$

Note that the variational procedure is of the Rayleigh-Ritz type with the basis functions being fixed and the stationary states arrived at by varying the coefficients $c_{L\kappa i\sigma}(\mathbf{k})$ [28]. A more detailed description will be given in the following section.

In closing this section, we turn to the determination of the core states. One way to do so is the so-called frozen-core approximation, which uses core states as arising from an atomic calculation without allowing them to respond to the changes of the valence states coming with the formation of chemical bonds between the atoms during the iteration towards self-consistency. This offers the advantage that the large core state energies are fixed, which makes the evaluation of small total energy differences as they arise, e.g., in frozen-phonon calculations, much easier. Nevertheless, in the ASW method we opt for the correct approach and evaluate the core states from the same radial Schrödinger equation as used for the valence states, i.e. from (2.1.14) or (2.1.21). Since these equations contain the actual intraatomic potential

the core states feel any changes of the potential due to the valence states and rearrange their shape during the iterations towards self-consistency. The ASW method thus belongs to the so-called all-electron methods.

Denoting the radial part of the core states as $\varphi_{nli\sigma}(E_{nli\sigma}, r_{\mu i})$, where n is the principal quantum number, we write down the radial Schrödinger equation

$$\begin{aligned} & \left[-\frac{1}{r_{\mu i}} \frac{\partial^2}{\partial r_{\mu i}^2} r_{\mu i} + \frac{l(l+1)}{r_{\mu i}^2} + v_{i\sigma}^{MT}(r_{\mu i}) - v_{MTZ} - E_{nli\sigma} \right] \varphi_{nli\sigma}(E_{nli\sigma}, r_{\mu i}) \\ &= \left[-\frac{1}{r_{\mu i}} \frac{\partial^2}{\partial r_{\mu i}^2} r_{\mu i} + \frac{l(l+1)}{r_{\mu i}^2} + \hat{v}_{i\sigma}^{MT}(r_{\mu i}) - E_{nli\sigma} \right] \varphi_{nli\sigma}(E_{nli\sigma}, r_{\mu i}) = 0. \end{aligned} \quad (2.1.33)$$

As already mentioned above, the major difference to the valence states is due to the boundary conditions for the core states, which are also subject to the regularity of the radial function at the origin. Yet, in contrast to the valence states, both value and slope at the sphere boundary must vanish since the core states do not take part in the chemical bonding and thus are confined to their respective atomic sphere.

Methods using augmentation for the construction of basis functions offer the special advantage that by construction the valence states are orthogonal to the core states and thus an explicit orthogonalization is not necessary. This traces back to the fact that the radial parts of the basis functions, i.e. of the augmented Hankel and Bessel functions, obey the same radial Schrödinger equation as the radial parts of the core states. As a consequence, the radial overlap integral is just the Wronskian of the two functions involved [52, 55] (see also (3.3.14)). We thus obtain, e.g., for the augmented Hankel function

$$\begin{aligned} & (E_{l\kappa i\sigma}^{(H)} - E_{nli\sigma}) \int_0^{s_i} dr_{\mu i} r_{\mu i}^2 \tilde{h}_{l\kappa\sigma}(r_{\mu i}) \varphi_{nli\sigma}(E_{nli\sigma}, r_{\mu i}) \\ &= W\{r_{\mu i} \tilde{h}_{l\kappa\sigma}(r_{\mu i}), r_{\mu i} \varphi_{nli\sigma}(E_{nli\sigma}, r_{\mu i}) r_{\mu i}\} \Big|_0^{s_i}. \end{aligned} \quad (2.1.34)$$

The Wronskian in turn is defined by

$$\begin{aligned} & W\{r_{\mu i} \tilde{h}_{l\kappa\sigma}(r_{\mu i}), r_{\mu i} \varphi_{nli\sigma}(E_{nli\sigma}, r_{\mu i}) r_{\mu i}\} \\ &= r_{\mu i}^2 \tilde{h}_{l\kappa\sigma}(r_{\mu i}) \frac{\partial}{\partial r_{\mu i}} \varphi_{nli\sigma}(E_{nli\sigma}, r_{\mu i}) - r_{\mu i}^2 \varphi_{nli\sigma}(E_{nli\sigma}, r_{\mu i}) \frac{\partial}{\partial r_{\mu i}} \tilde{h}_{l\kappa\sigma}(r_{\mu i}). \end{aligned} \quad (2.1.35)$$

Combining (2.1.34) and (2.1.35) we find that the contribution to the integral from the origin vanishes due to the regularity of all the functions involved. In contrast, at the sphere boundary $r_{\mu i} = s_i$ the core states do not contribute because of their values and slopes being zero. Since the Hankel energy $E_{l\kappa i\sigma}^{(H)}$ is always higher than any of the core state energies we arrive at the conclusion that the integral in (2.1.34) vanishes. The same holds for the augmented Bessel function and thus the core states are orthogonal to the valence states. Note that this has been achieved just by augmentation without any explicit orthogonalization procedure.

2.2 The Secular Matrix

With the basis functions at hand we proceed to determining the coefficients entering the expansion (2.1.31) of the ground state wave function in terms of the Bloch-summed basis functions (2.1.30). Eventually, these coefficients grow out of the Rayleigh-Ritz variational procedure built on the minimization of the total energy with respect to the many-body wave function. Within the Hartree- and Hartree-Fock schemes the many-body wave function is expressed in terms of the single-particle wave functions and, hence, the variational procedure leads directly to single-particle equations. This is different in density functional theory, where the variational principle is initially formulated in terms of the density. However, by reintroducing single-particle states and by formally identifying the density of the interacting many-body system with that of a fictitious non-interacting system built on these single-particle states, Kohn and Sham were able to derive a set of single-particle Schrödinger-like equations,

$$[H_\sigma - \varepsilon_{\mathbf{k}\sigma}]|\psi_{\mathbf{k}\sigma}\rangle = 0, \quad (2.2.1)$$

with the effective single-particle Hamiltonian

$$H_\sigma = -\Delta + v_\sigma(\mathbf{r}) - v_{MTZ} \quad (2.2.2)$$

already known from (2.1.1). Here, we have explicitly referred the potential to the muffin-tin zero and implied Bloch symmetry by attaching the \mathbf{k} -label to the single-particle energies and states. Within the variational principle the single-particle energies $\varepsilon_{\mathbf{k}\sigma}$ are just Lagrange multipliers, which guarantee normalization of the single-particle wave function $\psi_{\mathbf{k}\sigma}$. We thus arrive at the Euler-Lagrange variational equation

$$\delta[\langle\psi_{\mathbf{k}\sigma}|H_\sigma|\psi_{\mathbf{k}\sigma}\rangle - \varepsilon_{\mathbf{k}\sigma}\langle\psi_{\mathbf{k}\sigma}|\psi_{\mathbf{k}\sigma}\rangle] = 0. \quad (2.2.3)$$

In writing this expression we have implicitly assumed that the Hamiltonian is diagonal in spin. In particular, this implies the neglect of spin-orbit coupling. In addition, the decoupling of the spin states is based on the assumption that the system possesses a global spin quantization axis. As a consequence, we exclude those cases, which show a more general spin arrangement and which are covered by the so-called “non-collinear” ASW method [46, 47, 72].

Next, defining a bra-ket notation via

$$|L\kappa i\rangle^\infty := D_{L\kappa\sigma}^\infty(\mathbf{r}_i, \mathbf{k}) \quad (2.2.4)$$

for the Bloch-summed basis functions and using the expansion (2.1.31) of the wave function in terms of basis functions we rewrite (2.2.3) as

$$\delta \left[\sum_{L\kappa_1 i} \sum_{L'\kappa_2 j} c_{L\kappa_1 i \sigma}^*(\mathbf{k}) c_{L'\kappa_2 j \sigma}(\mathbf{k}) [\langle L\kappa_1 i | H_\sigma | L'\kappa_2 j \rangle_c^\infty - \varepsilon_{\mathbf{k}\sigma} \langle L\kappa_1 i | L'\kappa_2 j \rangle_c^\infty] \right] = 0. \quad (2.2.5)$$

Here, the matrix elements are real-space integrals and the index c indicates integration over the unit cell. Since within a linear method the energy corresponding to the state (2.1.31) can be minimized only by variation of the expansion coefficients we differentiate (2.2.5) with respect to $c_{L'\kappa_2j\sigma}(\mathbf{k})$ or else with respect to $c_{L\kappa_1i\sigma}^*(\mathbf{k})$ and arrive at the linear equation system

$$\sum_{L'\kappa_2j} c_{L'\kappa_2j\sigma}(\mathbf{k}) [\langle L\kappa_1i | H_\sigma | L'\kappa_2j \rangle_c^\infty - \varepsilon_{\mathbf{k}\sigma} \langle L\kappa_1i | L'\kappa_2j \rangle_c^\infty] = 0. \quad (2.2.6)$$

It allows to determine the band energies $\varepsilon_{\mathbf{k}n\sigma}$ from the condition that the coefficient determinant has to vanish for (2.2.6) to have a nontrivial solution. Here n labels the N different solutions, where N is the number of basis functions included in the expansion (2.1.31) and, hence, the rank of the coefficient matrix. In addition, the solution of (2.2.6) yields the wave function $\psi_{\mathbf{k}n\sigma}$ in terms of the expansion coefficients $c_{L\kappa_1i\sigma}(\mathbf{k})$ of the respective band. The generalized eigenvalue problem posed by (2.2.6) can be easily transformed into a standard eigenvalue problem with the help of the Cholesky decomposition, which is equivalent to a Gram-Schmidt orthogonalization. Obviously, it can be written as

$$(\mathcal{H} - \varepsilon \mathcal{S})\mathbf{C} = \mathbf{0}, \quad (2.2.7)$$

where \mathcal{H} and \mathcal{S} denote the Hamiltonian and overlap matrix, respectively. The latter is not necessarily the unit matrix since the basis functions usually are not orthonormalized. However, since the overlap matrix is positive definite, it can be decomposed into the product of an upper and a lower triangular matrices [63],

$$\mathcal{S} = \mathcal{U}^+ \mathcal{U}, \quad (2.2.8)$$

where \mathcal{U} is an upper triangular matrix. Inserting this into (2.2.7) we arrive at the standard eigenvalue problem

$$[(\mathcal{U}^+)^{-1} \mathcal{H} (\mathcal{U})^{-1} - \varepsilon \mathcal{E}] \mathcal{U} \mathbf{C} = \mathbf{0}, \quad (2.2.9)$$

where \mathcal{E} is the unit matrix. This standard eigenvalue problem can be routinely solved by mathematical-library routines but needs a backtransformation of the eigenvectors to those of the original generalized eigenvalue problem. Nowadays, there exist even library routines for the latter problem and we do not have to care about the details of the Cholesky decomposition.

Having sketched the general procedure for setting up and diagonalizing the secular matrix entering (2.2.6) we will, on the remaining pages of this section, derive the explicit form of the elements of both the Hamiltonian and overlap matrix. To this end, we complement (2.2.4) by the definition of a bra-ket notation for the Bloch-summed envelope function

$$|L\kappa i\rangle := D_{L\kappa}(\mathbf{r}_i, \mathbf{k}). \quad (2.2.10)$$

We may then write the general element of the Hamiltonian matrix as

$$\begin{aligned} & \langle L\kappa_1 i | H_\sigma | L'\kappa_2 j \rangle_c^\infty \\ &= \langle L\kappa_1 i | -\Delta | L'\kappa_2 j \rangle_c \\ &+ \sum_m [\langle L\kappa_1 i | H_\sigma | L'\kappa_2 j \rangle_{A(m)}^\infty - \langle L\kappa_1 i | -\Delta | L'\kappa_2 j \rangle_{A(m)}], \end{aligned} \quad (2.2.11)$$

where the integrals containing $-\Delta$ are to be taken with the non-augmented envelope functions and the index $A(m)$ denotes integration over the atomic sphere centered at τ_m . However, (2.2.11) is still valid for any other choice of sphere radii.

As it stands, (2.2.11) seems to be an *ad hoc* approach to the Hamiltonian matrix elements. Obviously, it is a first step beyond a formulation solely based on the ASA, which would only include the first term in square brackets without taking the integrals with the Laplacian operator into account. Insofar, (2.2.11) is well grounded. The terms adding to the pure ASA matrix elements considerably increase the accuracy of the method. In the LMTO method these terms are explicitly distinguished from the ASA terms and are referred to as the “combined correction”. This is different in the ASW method, where they are built in from the very beginning. However, while a formal justification of (2.2.11) is still missing, we will make up for this in Sect. 4.2. For the time being, we note the similarity to the alternative representation of the effective single-particle potential as given in the second line of (2.1.2). There we separated the potential into a so-called pseudo part, which displayed, if at all, only small spatial variations and extended over all space, and additional local parts, which were confined to the atomic spheres and contained the intraatomic strong variations of the potential. Equation (2.2.11) is in the same spirit with the first term being the pseudo contribution and the square brackets covering the local add-ons.

In order to evaluate the integral (2.2.11) we use the fact that in the respective regions of integration the functions entering are eigenfunctions of either the full Hamiltonian H_σ or else the free-electron Hamiltonian $-\Delta$. We may therefore reduce the integrals with these operators to overlap integrals times the respective eigenenergies and note, e.g., for the Laplacian operator

$$\langle L\kappa_1 i | -\Delta | L'\kappa_2 j \rangle_c = \kappa_2^2 \langle L\kappa_1 i | L'\kappa_2 j \rangle_c. \quad (2.2.12)$$

We are now able to evaluate the integrals extending over the atomic spheres to be built with the full Hamiltonian. Using (2.1.30) for the Bloch-summed basis function we write

$$\begin{aligned} & \infty \langle L\kappa_1 i | H_\sigma | L'\kappa_2 j \rangle_{A(m)}^\infty \\ &= \delta_{im} E_{l\kappa_2 j \sigma}^{(H)} \langle \tilde{H}_{L\kappa_1 \sigma} | \tilde{H}_{L'\kappa_2 \sigma} \rangle_{A(m)} \delta_{LL'} \delta_{mj} \\ &+ \delta_{im} E_{l''\kappa_2 m \sigma}^{(J)} \langle \tilde{H}_{L\kappa_1 \sigma} | \tilde{J}_{L''\kappa_2 \sigma} \rangle_{A(m)} \delta_{LL''} B_{L''L'\kappa_2}(\tau_m - \tau_j, \mathbf{k}) \\ &+ B_{L''L\kappa_1}^*(\tau_m - \tau_i, \mathbf{k}) E_{l'\kappa_2 m \sigma}^{(H)} \delta_{L''L'} \langle \tilde{J}_{L''\kappa_1 \sigma} | \tilde{H}_{L'\kappa_2 \sigma} \rangle_{A(m)} \delta_{mj} \\ &+ \sum_{L''} \sum_{L'''} B_{L''L\kappa_1}^*(\tau_m - \tau_i, \mathbf{k}) E_{l'''\kappa_2 m \sigma}^{(J)} \langle \tilde{J}_{L''\kappa_1 \sigma} | \tilde{J}_{L'''\kappa_2 \sigma} \rangle_{A(m)} \\ &\quad \times \delta_{L''L'''} B_{L''L'\kappa_2}(\tau_m - \tau_j, \mathbf{k}) \\ &= \delta_{im} E_{l\kappa_2 j \sigma}^{(H)} \langle \tilde{H}_{L\kappa_1 \sigma} | \tilde{H}_{L\kappa_2 \sigma} \rangle_{A(m)} \delta_{LL'} \delta_{mj} \\ &+ \delta_{im} E_{l\kappa_2 m \sigma}^{(J)} \langle \tilde{H}_{L\kappa_1 \sigma} | \tilde{J}_{L\kappa_2 \sigma} \rangle_{A(m)} B_{LL'\kappa_2}(\tau_m - \tau_j, \mathbf{k}) \\ &+ B_{L'L\kappa_1}^*(\tau_m - \tau_i, \mathbf{k}) E_{l'\kappa_2 m \sigma}^{(H)} \langle \tilde{J}_{L'\kappa_1 \sigma} | \tilde{H}_{L'\kappa_2 \sigma} \rangle_{A(m)} \delta_{mj} \\ &+ \sum_{L''} B_{L''L\kappa_1}^*(\tau_m - \tau_i, \mathbf{k}) E_{l''\kappa_2 m \sigma}^{(J)} \langle \tilde{J}_{L''\kappa_1 \sigma} | \tilde{J}_{L''\kappa_2 \sigma} \rangle_{A(m)} \\ &\quad \times B_{L''L'\kappa_2}(\tau_m - \tau_j, \mathbf{k}). \end{aligned} \quad (2.2.13)$$

Here we have taken into account the Schrödinger equations (2.1.14) and (2.1.21) as well as the orthogonality of the spherical harmonics, which leaves us with the Kronecker- δ 's with respect to angular momenta and reduces the intraatomic integrals to only their radial contributions. Of the radial integrals those, which contain only one type of function for $\kappa_1^2 = \kappa_2^2$, are calculated numerically. These integrals are defined in (6.1.1) and (6.1.2) as $S_{l\kappa i\sigma}^{(H)} = \langle \tilde{H}_{L\kappa\sigma} | \tilde{H}_{L\kappa\sigma} \rangle_{A(i)}$ and $S_{l\kappa i\sigma}^{(J)} = \langle \tilde{J}_{L\kappa\sigma} | \tilde{J}_{L\kappa\sigma} \rangle_{A(i)}$ and designated as the Hankel and Bessel integrals, respectively. The mixed integrals $\langle \tilde{H}_{L\kappa_1\sigma} | \tilde{H}_{L\kappa_2\sigma} \rangle_{A(m)}$, $\langle \tilde{H}_{L\kappa_1\sigma} | \tilde{J}_{L\kappa_2\sigma} \rangle_{A(m)}$ and $\langle \tilde{J}_{L\kappa_1\sigma} | \tilde{J}_{L\kappa_2\sigma} \rangle_{A(m)}$ are then expressed in terms of the Hankel and Bessel energies and integrals with the help of the identities derived in Sect. 6.1.

In (2.2.13) we distinguish three different types of integrals. They are called one-, two-, and three-center integrals depending on the number of sites involved, where counting includes the site of the atomic sphere, over which the integration extends. One-center integrals contain only augmented Hankel functions, two-center integrals both a Hankel and a Bessel function and, finally, three-center integrals contain only augmented Bessel functions. Note that due to the orthogonality of the spherical harmonics the limitation to the low- l Bessel functions is exact for the two-center integrals. In contrast, the three-center integrals still contain an in principle infinite summation over L'' . However, in this respect the formulation (2.2.11) of the general matrix element offers a distinct advantage. Due to this formulation, three-center integrals enter only in the square bracket term on the right-hand side of (2.2.11) and they always enter in combination with the corresponding integrals built with the envelope functions. Since for high angular momenta the muffin-tin potential in the Hamiltonian H_σ is dominated by the centrifugal term the augmented functions become identical to the envelope functions. As a consequence, the difference of the two terms in square brackets vanishes and it is well justified to omit the difference of three-center terms already for quite low angular momenta. This is why the angular momentum cutoff for the intermediate waves, l_{int} , can be fixed to a rather low value, which, in practice, is $l_{low} + 1$.

The second term in the square bracket on the right-hand side of (2.2.11), i.e. the integral over the atomic spheres, which contains envelope rather than augmented functions, simply results from (2.2.13) by replacing the Hankel and Bessel energies by κ_2^2 and the augmented functions by the envelope functions. We thus note

$$\begin{aligned}
 & \langle L\kappa_1 i | -\Delta | L'\kappa_2 j \rangle_{A(m)} \\
 &= \delta_{im} \kappa_2^2 \langle H_{L\kappa_1\sigma} | H_{L\kappa_2\sigma} \rangle_{A(m)} \delta_{LL'} \delta_{mj} \\
 &+ \delta_{im} \kappa_2^2 \langle H_{L\kappa_1\sigma} | J_{L\kappa_2\sigma} \rangle_{A(m)} B_{LL'\kappa_2}(\tau_m - \tau_j, \mathbf{k}) \\
 &+ B_{L'L\kappa_1}^*(\tau_m - \tau_i, \mathbf{k}) \kappa_2^2 \langle J_{L'\kappa_1\sigma} | H_{L'\kappa_2\sigma} \rangle_{A(m)} \delta_{mj} \\
 &+ \sum_{L''} B_{L''L\kappa_1}^*(\tau_m - \tau_i, \mathbf{k}) \kappa_2^2 \langle J_{L''\kappa_1\sigma} | J_{L''\kappa_2\sigma} \rangle_{A(m)} B_{L''L'\kappa_2}(\tau_m - \tau_j, \mathbf{k}),
 \end{aligned} \tag{2.2.14}$$

where again we have used the orthogonality of the spherical harmonics. The radial integrals are calculated using the identities given in Sect. 3.8.

Obviously, difficulties may arise from the first, second, and third term on the right-hand side of (2.2.14) due to the singularity of the Hankel envelope functions at their respective origins. While the product of a Hankel envelope function and a Bessel envelope function can still be integrated, the difficulty remains in the first term. However, as we will see in the next paragraph, this integral is only formally included here in order to compensate part of the first term of (2.2.11), which holds the integral over the product of two Hankel envelope functions extending over all space. In particular, if both basis functions are centered at the same site, the integration over the product of the two Hankel envelope functions centered at this site extends only over the region outside their on-center sphere and the singularities do not enter.

Next, we turn to the first term in (2.2.11), which, according to (2.2.12), can again be reduced to an overlap integral. Calculation of the latter is likewise the subject of Sect. 3.8. In particular, (3.8.39) gives the overlap integral of two Bloch-summed envelope functions extending over the interstitial region, which is identical to the difference of the first term and the second term in square brackets on the right-hand side of (2.2.11). Using these results and combining (2.2.11) to (2.2.13) as well as (3.8.39) we are eventually able to write down the general matrix element of the Hamiltonian as

$$\begin{aligned}
& \infty \langle L\kappa_1 i | H_\sigma | L'\kappa_2 j \rangle_c^\infty \\
&= [E_{l\kappa_2 j \sigma}^{(H)} \langle \tilde{H}_{L\kappa_1 \sigma} | \tilde{H}_{L\kappa_2 \sigma} \rangle_{A(j)} + \kappa_2^2 \langle H_{L\kappa_1} | H_{L\kappa_2} \rangle'_{A(j)}] \delta_{LL'} \delta_{ij} \\
&+ \frac{\kappa_2^2}{\kappa_2^2 - \kappa_1^2} [B_{LL'\kappa_2}(\boldsymbol{\tau}_i - \boldsymbol{\tau}_j, \mathbf{k}) - B_{L'L\kappa_1}^*(\boldsymbol{\tau}_j - \boldsymbol{\tau}_i, \mathbf{k})] (1 - \delta(\kappa_1^2 - \kappa_2^2)) \\
&+ \kappa_2^2 \dot{B}_{LL'\kappa_1}(\boldsymbol{\tau}_i - \boldsymbol{\tau}_j, \mathbf{k}) \delta(\kappa_1^2 - \kappa_2^2) \\
&+ [E_{l\kappa_2 i \sigma}^{(J)} \langle \tilde{H}_{L\kappa_1 \sigma} | \tilde{J}_{L\kappa_2 \sigma} \rangle_{A(i)} - \kappa_2^2 \langle H_{L\kappa_1} | J_{L\kappa_2} \rangle_{A(i)}] B_{LL'\kappa_2}(\boldsymbol{\tau}_i - \boldsymbol{\tau}_j, \mathbf{k}) \\
&+ B_{L'L\kappa_1}^*(\boldsymbol{\tau}_j - \boldsymbol{\tau}_i, \mathbf{k}) [E_{l'\kappa_2 j \sigma}^{(H)} \langle \tilde{J}_{L'\kappa_1 \sigma} | \tilde{H}_{L'\kappa_2 \sigma} \rangle_{A(j)} - \kappa_2^2 \langle J_{L'\kappa_1} | H_{L'\kappa_2} \rangle_{A(j)}] \\
&+ \sum_m \sum_{L''} B_{L''L\kappa_1}^*(\boldsymbol{\tau}_m - \boldsymbol{\tau}_i, \mathbf{k}) \\
&\times [E_{l''\kappa_2 m \sigma}^{(J)} \langle \tilde{J}_{L''\kappa_1 \sigma} | \tilde{J}_{L''\kappa_2 \sigma} \rangle_{A(m)} - \kappa_2^2 \langle J_{L''\kappa_1} | J_{L''\kappa_2} \rangle_{A(m)}] \\
&\times B_{L''L'\kappa_2}(\boldsymbol{\tau}_m - \boldsymbol{\tau}_j, \mathbf{k}). \tag{2.2.15}
\end{aligned}$$

In particular, we point to the two terms in the first square bracket, which comprise the integral over the product of two augmented Hankel functions extending over their on-center sphere and the integral over the product of two Hankel envelope functions extending over all space outside the on-center sphere, as indicated by the prime. Thus, as mentioned in connection with (2.2.14), the singularities of the Hankel envelope functions do not enter.

It is useful to define the following abbreviations for the one-, two-, and three-center contributions

$$X_{L\kappa_1 \kappa_2 i \sigma}^{(H,1)} = E_{l\kappa_2 i \sigma}^{(H)} \langle \tilde{H}_{L\kappa_1 \sigma} | \tilde{H}_{L\kappa_2 \sigma} \rangle_{A(i)} + \kappa_2^2 \langle H_{L\kappa_1} | H_{L\kappa_2} \rangle'_{A(i)}, \tag{2.2.16}$$

$$X_{L\kappa_1\kappa_2i\sigma}^{(H,2)} = E_{l\kappa_2i\sigma}^{(J)} \langle \tilde{H}_{L\kappa_1\sigma} | \tilde{J}_{L\kappa_2\sigma} \rangle_{A(i)} - \kappa_2^2 \langle H_{L\kappa_1} | J_{L\kappa_2} \rangle_{A(i)} + \frac{\kappa_2^2}{\kappa_2^2 - \kappa_1^2} (1 - \delta(\kappa_1^2 - \kappa_2^2)), \quad (2.2.17)$$

$$X_{L\kappa_1\kappa_2i\sigma}^{(H,3)} = E_{l\kappa_2i\sigma}^{(J)} \langle \tilde{J}_{L\kappa_1\sigma} | \tilde{J}_{L\kappa_2\sigma} \rangle_{A(i)} - \kappa_2^2 \langle J_{L\kappa_1} | J_{L\kappa_2} \rangle_{A(i)}. \quad (2.2.18)$$

Furthermore, combining (2.2.17), (3.3.37), and (6.1.9) we derive the identity

$$E_{l\kappa_2i\sigma}^{(H)} \langle \tilde{J}_{L\kappa_1\sigma} | \tilde{H}_{L\kappa_2\sigma} \rangle_{A(i)} - \kappa_2^2 \langle J_{L\kappa_1} | H_{L\kappa_2} \rangle_{A(i)} - \frac{\kappa_2^2}{\kappa_2^2 - \kappa_1^2} (1 - \delta(\kappa_1^2 - \kappa_2^2)) = X_{L\kappa_2\kappa_1i\sigma}^{(H,2)} + \delta(\kappa_1^2 - \kappa_2^2), \quad (2.2.19)$$

which complements (2.2.17). The Hamiltonian matrix element then assumes the form

$$\begin{aligned} & \infty \langle L\kappa_1 i | H_\sigma | L' \kappa_2 j \rangle_c^\infty \\ &= X_{L\kappa_1\kappa_2i\sigma}^{(H,1)} \delta_{LL'} \delta_{ij} + \kappa_2^2 \dot{B}_{LL'\kappa_1}(\boldsymbol{\tau}_i - \boldsymbol{\tau}_j, \mathbf{k}) \delta(\kappa_1^2 - \kappa_2^2) \\ &+ X_{L\kappa_1\kappa_2i\sigma}^{(H,2)} B_{LL'\kappa_2}(\boldsymbol{\tau}_i - \boldsymbol{\tau}_j, \mathbf{k}) \\ &+ B_{L'L\kappa_1}^*(\boldsymbol{\tau}_j - \boldsymbol{\tau}_i, \mathbf{k}) (X_{L'\kappa_2\kappa_1j\sigma}^{(H,2)} + \delta(\kappa_1^2 - \kappa_2^2)) \\ &+ \sum_m \sum_{L''} B_{L''L\kappa_1}^*(\boldsymbol{\tau}_m - \boldsymbol{\tau}_i, \mathbf{k}) X_{L''\kappa_1\kappa_2m\sigma}^{(H,3)} B_{L''L'\kappa_2}(\boldsymbol{\tau}_m - \boldsymbol{\tau}_j, \mathbf{k}). \end{aligned} \quad (2.2.20)$$

Here we have, in addition, used the identity (6.1.8). Finally, working with cubic rather than spherical harmonics and, using the identity (3.7.18), we get for the Hamiltonian matrix element the final result

$$\begin{aligned} & \infty \langle L\kappa_1 i | H_\sigma | L' \kappa_2 j \rangle_c^\infty \\ &= X_{L\kappa_1\kappa_2i\sigma}^{(H,1)} \delta_{LL'} \delta_{ij} + \kappa_2^2 \dot{B}_{LL'\kappa_1}(\boldsymbol{\tau}_i - \boldsymbol{\tau}_j, \mathbf{k}) \delta(\kappa_1^2 - \kappa_2^2) \\ &+ X_{L\kappa_1\kappa_2i\sigma}^{(H,2)} B_{LL'\kappa_2}(\boldsymbol{\tau}_i - \boldsymbol{\tau}_j, \mathbf{k}) \\ &+ B_{LL'\kappa_1}(\boldsymbol{\tau}_i - \boldsymbol{\tau}_j, \mathbf{k}) (X_{L'\kappa_2\kappa_1j\sigma}^{(H,2)} + \delta(\kappa_1^2 - \kappa_2^2)) \\ &+ \sum_m \sum_{L''} B_{L''L\kappa_1}^*(\boldsymbol{\tau}_m - \boldsymbol{\tau}_i, \mathbf{k}) X_{L''\kappa_1\kappa_2m\sigma}^{(H,3)} B_{L''L'\kappa_2}(\boldsymbol{\tau}_m - \boldsymbol{\tau}_j, \mathbf{k}). \end{aligned} \quad (2.2.21)$$

With the Hamiltonian matrix element at hand evaluation of the elements of the overlap matrix turns out to be quite easy. In accordance with (2.2.11) these matrix elements are defined as

$$\begin{aligned} & \infty \langle L\kappa_1 i | L' \kappa_2 j \rangle_c^\infty \\ &= \langle L\kappa_1 i | L' \kappa_2 j \rangle_c \\ &+ \sum_m [\infty \langle L\kappa_1 i | L' \kappa_2 j \rangle_{A(m)}^\infty - \langle L\kappa_1 i | L' \kappa_2 j \rangle_{A(m)}]. \end{aligned} \quad (2.2.22)$$

Since all the functions entering this expression are eigenfunctions of either the full Hamiltonian H_σ or else the free-electron Hamiltonian $-\Delta$ we may fall back on the just derived results for the Hamiltonian matrix. To be specific, we start from (2.2.15) and replace all energies, which appear in a numerator, by unity. We thus obtain as an intermediate result for the general matrix element of the overlap matrix

$$\begin{aligned}
& \infty \langle L\kappa_1 i | L'\kappa_2 j \rangle_c^\infty \\
&= [\langle \tilde{H}_{L\kappa_1\sigma} | \tilde{H}_{L\kappa_2\sigma} \rangle_{A(j)} + \langle H_{L\kappa_1} | H_{L\kappa_2} \rangle'_{A(j)}] \delta_{LL'} \delta_{ij} \\
&+ \frac{1}{\kappa_2^2 - \kappa_1^2} [B_{LL'\kappa_2}(\boldsymbol{\tau}_i - \boldsymbol{\tau}_j, \mathbf{k}) - B_{L'L\kappa_1}^*(\boldsymbol{\tau}_j - \boldsymbol{\tau}_i, \mathbf{k})] (1 - \delta(\kappa_1^2 - \kappa_2^2)) \\
&+ \dot{B}_{LL'\kappa_1}(\boldsymbol{\tau}_i - \boldsymbol{\tau}_j, \mathbf{k}) \delta(\kappa_1^2 - \kappa_2^2) \\
&+ [\langle \tilde{H}_{L\kappa_1\sigma} | \tilde{J}_{L\kappa_2\sigma} \rangle_{A(i)} - \langle H_{L\kappa_1} | J_{L\kappa_2} \rangle_{A(i)}] B_{LL'\kappa_2}(\boldsymbol{\tau}_i - \boldsymbol{\tau}_j, \mathbf{k}) \\
&+ B_{L'L\kappa_1}^*(\boldsymbol{\tau}_j - \boldsymbol{\tau}_i, \mathbf{k}) [\langle \tilde{J}_{L'\kappa_1\sigma} | \tilde{H}_{L'\kappa_2\sigma} \rangle_{A(j)} - \langle J_{L'\kappa_1} | H_{L'\kappa_2} \rangle_{A(j)}] \\
&+ \sum_m \sum_{L''} B_{L''L\kappa_1}^*(\boldsymbol{\tau}_m - \boldsymbol{\tau}_i, \mathbf{k}) [\langle \tilde{J}_{L''\kappa_1\sigma} | \tilde{J}_{L''\kappa_2\sigma} \rangle_{A(m)} - \langle J_{L''\kappa_1} | J_{L''\kappa_2} \rangle_{A(m)}] \\
&\times B_{L''L'\kappa_2}(\boldsymbol{\tau}_m - \boldsymbol{\tau}_j, \mathbf{k}). \tag{2.2.23}
\end{aligned}$$

As before we abbreviate the one-, two-, and three-center contributions to the elements of the overlap matrix by

$$X_{L\kappa_1\kappa_2 i\sigma}^{(S,1)} = \langle \tilde{H}_{L\kappa_1\sigma} | \tilde{H}_{L\kappa_2\sigma} \rangle_{A(i)} + \langle H_{L\kappa_1} | H_{L\kappa_2} \rangle'_{A(i)}, \tag{2.2.24}$$

$$\begin{aligned}
X_{L\kappa_1\kappa_2 i\sigma}^{(S,2)} &= \langle \tilde{H}_{L\kappa_1\sigma} | \tilde{J}_{L\kappa_2\sigma} \rangle_{A(i)} - \langle H_{L\kappa_1} | J_{L\kappa_2} \rangle_{A(i)} \\
&+ \frac{1}{\kappa_2^2 - \kappa_1^2} (1 - \delta(\kappa_1^2 - \kappa_2^2)), \tag{2.2.25}
\end{aligned}$$

$$X_{L\kappa_1\kappa_2 i\sigma}^{(S,3)} = \langle \tilde{J}_{L\kappa_1\sigma} | \tilde{J}_{L\kappa_2\sigma} \rangle_{A(i)} - \langle J_{L\kappa_1} | J_{L\kappa_2} \rangle_{A(i)}. \tag{2.2.26}$$

Combining (2.2.23) to (2.2.26) we note the result

$$\begin{aligned}
& \infty \langle L\kappa_1 i | L'\kappa_2 j \rangle_c^\infty \\
&= X_{L\kappa_1\kappa_2 i\sigma}^{(S,1)} \delta_{LL'} \delta_{ij} + \dot{B}_{LL'\kappa_1}(\boldsymbol{\tau}_i - \boldsymbol{\tau}_j, \mathbf{k}) \delta(\kappa_1^2 - \kappa_2^2) \\
&+ X_{L\kappa_1\kappa_2 i\sigma}^{(S,2)} B_{LL'\kappa_2}(\boldsymbol{\tau}_i - \boldsymbol{\tau}_j, \mathbf{k}) + B_{L'L\kappa_1}^*(\boldsymbol{\tau}_j - \boldsymbol{\tau}_i, \mathbf{k}) X_{L'\kappa_2\kappa_1 j\sigma}^{(S,2)} \\
&+ \sum_m \sum_{L''} B_{L''L\kappa_1}^*(\boldsymbol{\tau}_m - \boldsymbol{\tau}_i, \mathbf{k}) X_{L''\kappa_1\kappa_2 m\sigma}^{(S,3)} B_{L''L'\kappa_2}(\boldsymbol{\tau}_m - \boldsymbol{\tau}_j, \mathbf{k}), \tag{2.2.27}
\end{aligned}$$

which for cubic harmonics reads as

$$\begin{aligned}
& \infty \langle L\kappa_1 i | L'\kappa_2 j \rangle_c^\infty \\
&= X_{L\kappa_1\kappa_2 i\sigma}^{(S,1)} \delta_{LL'} \delta_{ij} + \dot{B}_{LL'\kappa_1}(\boldsymbol{\tau}_i - \boldsymbol{\tau}_j, \mathbf{k}) \delta(\kappa_1^2 - \kappa_2^2) \\
&+ X_{L\kappa_1\kappa_2 i\sigma}^{(S,2)} B_{LL'\kappa_2}(\boldsymbol{\tau}_i - \boldsymbol{\tau}_j, \mathbf{k}) + B_{LL'\kappa_1}(\boldsymbol{\tau}_i - \boldsymbol{\tau}_j, \mathbf{k}) X_{L'\kappa_2\kappa_1 j\sigma}^{(S,2)} \\
&+ \sum_m \sum_{L''} B_{L''L\kappa_1}^*(\boldsymbol{\tau}_m - \boldsymbol{\tau}_i, \mathbf{k}) X_{L''\kappa_1\kappa_2 m\sigma}^{(S,3)} B_{L''L'\kappa_2}(\boldsymbol{\tau}_m - \boldsymbol{\tau}_j, \mathbf{k}). \tag{2.2.28}
\end{aligned}$$

By now, we have arrived at a formulation for the elements of the secular matrix, which offers several advantages. First off all, we have separated structural information from intraatomic information by writing each term as a structure constant times intraatomic radial integrals. The latter need to be calculated only once in an iteration before the time consuming loop over \mathbf{k} -points starts. Moreover, as can be read off from the definitions (2.2.16) to (2.2.18), (2.2.24) to (2.2.26) and (6.1.8), the intraatomic contributions depend exclusively on integrals over envelope functions, which can be performed analytically, as well as on the Hankel and Bessel energies $E_{l\kappa i\sigma}^{(H)}$ and $E_{l\kappa i\sigma}^{(J)}$ and on the Hankel and Bessel integrals $S_{l\kappa i\sigma}^{(H)}$ and $S_{l\kappa i\sigma}^{(J)}$. Hence, except for the crystal structure information, the secular matrix is completely specified by four numbers per basis state, which contain all information about the shape of the crystal potential. Second, the present formulation of the secular matrix allows for a very efficient computation. In practice, (2.2.21) and (2.2.28) enable for both a high degree of vectorization and low memory costs and thus contribute a lot to the high computational efficiency of the ASW method.

2.3 Electron Density

Having described the setup of ASW basis functions as well as of the secular matrix we next turn to the calculation of the spin-dependent electron density, which comprises contributions from both the valence and core electrons.

Within the framework of density functional theory, the spin-dependent valence electron density is given by

$$\rho_{val,\sigma}(\mathbf{r}) = \sum_{\mathbf{k}n} |\psi_{\mathbf{k}n\sigma}(\mathbf{r})|^2 \Theta(E_F - \varepsilon_{\mathbf{k}n\sigma}). \quad (2.3.1)$$

Here we have implied zero-temperature Fermi statistics by summing over the occupied states up to the Fermi energy E_F . Note that, according to the definition (2.2.2), the band energies $\varepsilon_{\mathbf{k}n\sigma}$ as well as the Fermi energy are referred to the muffin-tin zero, v_{MTZ} . The wave function is that defined by (2.1.31) with the coefficients determined by the solution of the generalized eigenvalue problem (2.2.7); n labels the different eigenstates. The spin-dependent electron density is then arrived at by combining (2.3.1) and (2.1.31) with the expression (2.1.30) for the ASW basis function. However, within the standard ASW method it is possible to follow a different route, which is based on the density of states and which will be used in the present context.

To this end, we first recall the fact that we started out from a muffin-tin potential in Sect. 2.1. For this reason, due to the self-consistency condition growing out of density functional theory the potential to be eventually extracted from the electron density also must be a muffin-tin potential. Hence, we may already reduce the electron density to a muffin-tin form. Within this so-called shape approximation it is sufficient to calculate only the spherical symmetric contributions inside the atomic spheres. However, the spherical symmetric valence electron density may be equally well extracted from the electronic density of states. It has been argued that this offers the additional advantage of an increased accuracy because the Rayleigh-Ritz

variational procedure gives higher accuracy to the eigenenergies than to the eigenfunctions [5, 6, 78].

Following the previous arguments, we concentrate from now on the spherical symmetric spin-dependent electron density within the atomic spheres. In addition, we strictly enforce the ASA, i.e. we ignore the interstitial region completely and treat the atomic spheres as non-overlapping. Note that at this point we lay ground for the systematic error of the total energy expression of the standard ASW method. This will be explicited in Sect. 2.4.

To be specific, we rewrite the wave function as given by (2.1.30) and (2.1.31) for the situation that the vector \mathbf{r} lies within an atomic sphere as

$$\psi_{\mathbf{k}\sigma}(\mathbf{r}) = \sum_{L\kappa i} [c_{L\kappa i\sigma}(\mathbf{k}) \tilde{H}_{L\kappa\sigma}(\mathbf{r}_i) + a_{L\kappa i\sigma}(\mathbf{k}) \tilde{J}_{L\kappa\sigma}(\mathbf{r}_i)], \quad (2.3.2)$$

where we have used the abbreviation (2.1.32) in the form

$$a_{L\kappa i\sigma}(\mathbf{k}) = \sum_{L'j} c_{L'\kappa j\sigma}(\mathbf{k}) B_{LL'\kappa}(\mathbf{r}_i - \mathbf{r}_j, \mathbf{k}). \quad (2.3.3)$$

Inserting this into (2.3.1) we get for the spin-dependent valence electron density

$$\rho_{val,\sigma}(\mathbf{r}) = \sum_i \rho_{val,i\sigma}(\mathbf{r}_i) \quad (2.3.4)$$

with the spherical symmetric part given by

$$\begin{aligned} & \rho_{val,i\sigma}(r_i) \\ &= \frac{1}{4\pi} \int d\Omega \rho_{val,i\sigma}(\mathbf{r}_i) \\ &= \frac{1}{4\pi} \int d\Omega \sum_{\mathbf{k}} \Theta(E_F - \varepsilon_{\mathbf{k}\sigma}) \\ & \quad \times \sum_L \left| \sum_{\kappa} (c_{L\kappa i\sigma}(\mathbf{k}) \tilde{H}_{L\kappa\sigma}(\mathbf{r}_i) + a_{L\kappa i\sigma}(\mathbf{k}) \tilde{J}_{L\kappa\sigma}(\mathbf{r}_i)) \right|^2 \\ &= \frac{1}{4\pi} \int d\Omega \int_{-\infty}^{E_F} dE \sum_{\mathbf{k}} \delta(E - \varepsilon_{\mathbf{k}\sigma}) \\ & \quad \times \sum_L \left| \sum_{\kappa} (c_{L\kappa i\sigma}(\mathbf{k}) \tilde{H}_{L\kappa\sigma}(\mathbf{r}_i) + a_{L\kappa i\sigma}(\mathbf{k}) \tilde{J}_{L\kappa\sigma}(\mathbf{r}_i)) \right|^2. \end{aligned} \quad (2.3.5)$$

Here we have formally absorbed the band index n into the \mathbf{k} -point label. Note that the sum over δ functions is just the electronic density of states

$$\rho_{\sigma}(E) = \sum_{\mathbf{k}} \delta(E - \varepsilon_{\mathbf{k}\sigma}). \quad (2.3.6)$$

The valence electron density as given by (2.3.5) thus arises as a sum over weighted or partial densities of states. This representation is based on the orthonormality of the spherical harmonics as well as the fact that within the ASA the overlap of the

atomic spheres is ignored. As a consequence, the valence electron density is diagonal in both the atomic sphere and the angular momentum index and can be written as a single sum over these indices.

Nevertheless, due to the energy linearization it is not straightforward to perform the energy integration on the right-hand side of (2.3.5). Instead of the augmented Hankel and Bessel functions, which inside their respective spheres are solutions of Schrödinger's equation for two particular energies (the Hankel and Bessel energies), we would seemingly need the full energy dependence of the wave function. Actually, as we will see below, the energy linearization leads a way out of this problem. Nevertheless, it pays to check what the valence electron density would look like if the full energy dependence were taken into account. For this reason, we take a sideglance at the KKR method [40, 43, 45, 50], where the wave function reads as

$$\psi_{\mathbf{k}\sigma E}(\mathbf{r}) = \sum_{Li} \beta_{Li\sigma}(\mathbf{k}) R_{l\sigma}(E, r_i) Y_L(\hat{\mathbf{r}}_i). \quad (2.3.7)$$

The functions $R_{l\sigma}(E, r_i)$ are normalized regular solutions of the radial Schrödinger equation (2.1.14) for energy E . Hence, they embrace the set of augmented Hankel and Bessel functions, which are solutions of the same radial equation albeit for only the Hankel and Bessel energies. The coefficients $\beta_{Li\sigma}(\mathbf{k})$ are equivalent to the expansion coefficients $c_{L\kappa i\sigma}(\mathbf{k})$ entering (2.1.31). Using the KKR wave function (2.3.7) we readily arrive at the following expression for the radial part of the valence electron density

$$\begin{aligned} \rho_{val,i\sigma}(r_i) &= \frac{1}{4\pi} \int d\Omega \rho_{val,i\sigma}(\mathbf{r}_i) \\ &= \frac{1}{4\pi} \sum_{\mathbf{k}} \sum_L |\beta_{Li\sigma}(\mathbf{k})|^2 R_{l\sigma}^2(E_\sigma(\mathbf{k}), r_i) \Theta(E_F - \varepsilon_{\mathbf{k}\sigma}) \\ &= \frac{1}{4\pi} \int_{-\infty}^{E_F} dE \sum_l \sum_{\mathbf{k}} \delta(E - \varepsilon_{\mathbf{k}\sigma}) \sum_m |\beta_{lmi\sigma}(\mathbf{k})|^2 R_{l\sigma}^2(E, r_i). \end{aligned} \quad (2.3.8)$$

In contrast to (2.3.5) this expression preserves the full energy dependence of the radial function and thus the energy integration can be easily performed. Using the decomposition of the norm of the wave functions into contributions from atomic spheres and angular momenta,

$$\int_{\Omega_c} d^3\mathbf{r} |\psi_{\mathbf{k}\sigma E}(\mathbf{r})|^2 = \sum_{lmi} |\beta_{lmi\sigma}(\mathbf{k})|^2 \stackrel{!}{=} 1, \quad (2.3.9)$$

we can define partial densities of states by

$$\rho_{li\sigma}(E) := \sum_{\mathbf{k}} \delta(E - \varepsilon_{\mathbf{k}\sigma}) \sum_m |\beta_{lmi\sigma}(\mathbf{k})|^2 \quad (2.3.10)$$

and obtain for the KKR valence electron density

$$\rho_{val,i\sigma}(r_i) = \frac{1}{4\pi} \int_{-\infty}^{E_F} dE \sum_l \rho_{li\sigma}(E) R_{l\sigma}^2(E, r_i). \quad (2.3.11)$$

This result will be useful in setting up the valence electron density with a linear basis set.

With the just derived representation of the KKR valence electron density in mind we turn back to the ASW method and aim at the definition of partial densities of states via the decomposition of the norm. The latter is obtained from the expansion (2.1.31) of the wave functions in terms of the basis functions as

$$\int_{\Omega_c} d^3\mathbf{r} |\psi_{\mathbf{k}\sigma}(\mathbf{r})|^2 = \sum_{L\kappa_1 i} \sum_{L'\kappa_2 j} c_{L\kappa_1 i\sigma}^*(\mathbf{k}) c_{L'\kappa_2 j\sigma}(\mathbf{k}) \langle L\kappa_1 i | L'\kappa_2 j \rangle_c^\infty. \quad (2.3.12)$$

Inserting into this expression (2.2.23) for the overlap matrix and using the definition (2.3.3) we get

$$\begin{aligned} & \int_{\Omega_c} d^3\mathbf{r} |\psi_{\mathbf{k}\sigma}(\mathbf{r})|^2 \\ &= \sum_{L\kappa_1 \kappa_2 i} \left[c_{L\kappa_1 i\sigma}^*(\mathbf{k}) c_{L\kappa_2 i\sigma}(\mathbf{k}) [\langle \tilde{H}_{L\kappa_1 \sigma} | \tilde{H}_{L\kappa_2 \sigma} \rangle_i + \langle H_{L\kappa_1} | H_{L\kappa_2} \rangle_i'] \right. \\ & \quad + c_{L\kappa_1 i\sigma}^*(\mathbf{k}) \sum_{L'j} c_{L'\kappa_2 j\sigma}(\mathbf{k}) \frac{1}{\kappa_2^2 - \kappa_1^2} \\ & \quad \times [B_{LL'\kappa_2}(\boldsymbol{\tau}_i - \boldsymbol{\tau}_j, \mathbf{k}) - B_{L'L\kappa_1}^*(\boldsymbol{\tau}_j - \boldsymbol{\tau}_i, \mathbf{k})] (1 - \delta(\kappa_1^2 - \kappa_2^2)) \\ & \quad + c_{L\kappa_1 i\sigma}^*(\mathbf{k}) \sum_{L'j} c_{L'\kappa_2 j\sigma}(\mathbf{k}) \dot{B}_{LL'\kappa_1}(\boldsymbol{\tau}_i - \boldsymbol{\tau}_j, \mathbf{k}) \delta(\kappa_1^2 - \kappa_2^2) \\ & \quad + c_{L\kappa_1 i\sigma}^*(\mathbf{k}) a_{L\kappa_2 i\sigma}(\mathbf{k}) [\langle \tilde{H}_{L\kappa_1 \sigma} | \tilde{J}_{L\kappa_2 \sigma} \rangle_i - \langle H_{L\kappa_1} | J_{L\kappa_2} \rangle_i] \\ & \quad + a_{L\kappa_1 i\sigma}^*(\mathbf{k}) c_{L\kappa_2 i\sigma}(\mathbf{k}) [\langle \tilde{J}_{L\kappa_1 \sigma} | \tilde{H}_{L\kappa_2 \sigma} \rangle_i - \langle J_{L\kappa_1} | H_{L\kappa_2} \rangle_i] \\ & \quad \left. + a_{L\kappa_1 i\sigma}^*(\mathbf{k}) a_{L\kappa_2 i\sigma}(\mathbf{k}) [\langle \tilde{J}_{L\kappa_1 \sigma} | \tilde{J}_{L\kappa_2 \sigma} \rangle_i - \langle J_{L\kappa_1} | J_{L\kappa_2} \rangle_i] \right]. \quad (2.3.13) \end{aligned}$$

As already mentioned in the previous sections, the Hankel and Bessel functions are included up to l_{low} and l_{int} , respectively. Note that (2.3.13) is the exact representation of the norm. However, it does not allow for a straightforward decomposition into partial densities of states due to the double sum in the second and third term on the right-hand side. These terms originate from the so-called “combined correction” terms, i.e. from the difference of the first term and the second term in square brackets on the right-hand side of (2.2.11). Since we already opted for the ASA in the present context we replace the exact expression by the following ASA expression for the norm

$$\begin{aligned} \int_{\Omega_c} d^3\mathbf{r} |\psi_{\mathbf{k}\sigma}(\mathbf{r})|^2 &= \sum_{L\kappa_1 \kappa_2 i} [c_{L\kappa_1 i\sigma}^*(\mathbf{k}) c_{L\kappa_2 i\sigma}(\mathbf{k}) \langle \tilde{H}_{L\kappa_1 \sigma} | \tilde{H}_{L\kappa_2 \sigma} \rangle_i \\ & \quad + c_{L\kappa_1 i\sigma}^*(\mathbf{k}) a_{L\kappa_2 i\sigma}(\mathbf{k}) \langle \tilde{H}_{L\kappa_1 \sigma} | \tilde{J}_{L\kappa_2 \sigma} \rangle_i \\ & \quad + a_{L\kappa_1 i\sigma}^*(\mathbf{k}) c_{L\kappa_2 i\sigma}(\mathbf{k}) \langle \tilde{J}_{L\kappa_1 \sigma} | \tilde{H}_{L\kappa_2 \sigma} \rangle_i \\ & \quad + a_{L\kappa_1 i\sigma}^*(\mathbf{k}) a_{L\kappa_2 i\sigma}(\mathbf{k}) \langle \tilde{J}_{L\kappa_1 \sigma} | \tilde{J}_{L\kappa_2 \sigma} \rangle_i] + \Delta_\sigma(\mathbf{k}) \end{aligned}$$

$$\begin{aligned}
& =: \sum_{li} q_{li\sigma}(\mathbf{k}) \\
& \stackrel{!}{=} 1.
\end{aligned} \tag{2.3.14}$$

Here we have added a small quantity $\Delta_\sigma(\mathbf{k})$, which accounts for the difference between the expressions (2.3.13) and (2.3.14). Thus, it can in principle be calculated exactly. Yet, since this quantity makes only a small contribution to the norm it is omitted in practice and the resulting deviation of the norm from unity is cured by a renormalization of the remaining terms in (2.3.14).

As indicated in the second but last line of (2.3.14) we then arrive at the desired unique decomposition of the norm, which still allows to define \mathbf{k} -dependent partial occupation numbers. Moreover, we now have a simple recipe for the calculation of partial densities of states at hand, which read as

$$\rho_{li\sigma}(E) := \sum_{\mathbf{k}} \delta(E - \varepsilon_{\mathbf{k}\sigma}) q_{li\sigma}(\mathbf{k}). \tag{2.3.15}$$

Still, we are not able to perform the energy integration needed for the calculation of the spin-dependent valence electron density. In order to do so we would need the full energy dependence of the radial function, which in case of the KKR method is contained in the solution $R_{l\sigma}(E, r_j)$ of the radial Schrödinger equation. However, we point out that the full energy dependence is not really omitted in a linear method but is just replaced by a linear function [5, 69, 78]. Under the assumption of a perfectly linear dependence the partial density of states would be completely specified by its first three moments, which are defined by

$$M_{li\sigma}^{(k)} = \int_{-\infty}^{E_F} dE E^k \rho_{li\sigma}(E), \quad k = 0, 1, 2. \tag{2.3.16}$$

Even if small deviations from the linear behavior are included it will be sufficient to take additionally the fourth moment into account. This allows to define a new expression for the density of states

$$\tilde{\rho}_{li\sigma}(E) := \sum_{\alpha=1}^2 \delta(E - E_{li\sigma}^{(\alpha)}) Q_{li\sigma}^{(\alpha)}, \tag{2.3.17}$$

where the two energies $E_{li\sigma}^{(\alpha)}$ and the particle numbers $Q_{li\sigma}^{(\alpha)}$ are subject to the condition that they yield the same first four moments as the true density of states does, i.e.

$$\sum_{\alpha=1}^2 (E_{li\sigma}^{(\alpha)})^k Q_{li\sigma}^{(\alpha)} \stackrel{!}{=} \int_{-\infty}^{E_F} dE E^k \rho_{li\sigma}(E), \quad k = 0, 1, 2, 3. \tag{2.3.18}$$

The calculation of the moments of the partial densities of states as well as the details of the moment analysis (2.3.18) are the subject of Sects. 6.2 and 6.4, respectively.

Finally, with the true density of states replaced by (2.3.17) we arrive at the representation of the spin-dependent valence electron density as

$$\rho_{val,i\sigma}(r_i) = \frac{1}{4\pi} \sum_l \sum_{\alpha=1}^2 Q_{li\sigma}^{(\alpha)} R_{l\sigma}^2(E_{li\sigma}^{(\alpha)}, r_i) = \sum_l \rho_{val,li\sigma}(r_i). \quad (2.3.19)$$

It does not require the full energy dependence of the solution of the radial Schrödinger equation. Instead, we have to solve this equation for two energies only. Nevertheless, the first four moments of the true density of states are fully reproduced.

The previous results reveal an additional “symmetry” of the standard ASW method. Obviously, the intraatomic valence electron density by now is completely specified by only two energies $E_{li\sigma}^{(\alpha)}$ and particle numbers $Q_{li\sigma}^{(\alpha)}$. In return, as outlined at the end of Sect. 2.2, specification of the secular matrix likewise required four quantities per orbital, namely, the Hankel and Bessel energies and integrals. As a consequence, the iteration process can be cut into two parts. While the band calculation starts from the Hankel and Bessel energies and integrals and returns the above energies $E_{li\sigma}^{(\alpha)}$ and particle numbers $Q_{li\sigma}^{(\alpha)}$ things are reversed for the intraatomic calculations. Eventually, this bouncing back and forth of different quantities allows for an additional speedup of the method, which will be outlined in more detail in the following section.

Having performed the calculation of the valence electron density we turn to the core electrons. Their density arises from a sum over all core states, which have wave functions $\varphi_{nli\sigma}(E_{nli\sigma}, r_i)$ and energies $E_{nli\sigma}$ resulting from the radial Schrödinger equation (2.1.33) subject to the conditions of vanishing value and slope at the sphere boundary. Hence, we get for the spin-dependent core electron density

$$\begin{aligned} \rho_{core,\sigma}(\mathbf{r}) &= \sum_i \rho_{core,\sigma}(\mathbf{r}_i) = \sum_{nlmi} \varphi_{nli\sigma}^2(E_{nli\sigma}, r_i) |Y_L(\hat{\mathbf{r}}_i)|^2 \\ &= \sum_{nli} \frac{2l+1}{4\pi} \varphi_{nli\sigma}^2(E_{nli\sigma}, r_i) \\ &= \sum_i \rho_{core,\sigma}(r_i). \end{aligned} \quad (2.3.20)$$

Finally, combining (2.3.19) and (2.3.20) we arrive at the following result for the spin-dependent electron density

$$\rho_{el,\sigma}(\mathbf{r}) = \sum_i (\rho_{val,\sigma}(\mathbf{r}_i) + \rho_{core,\sigma}(\mathbf{r}_i)) =: \sum_i \rho_{el,\sigma}(\mathbf{r}_i). \quad (2.3.21)$$

2.4 The Effective Potential

In order to close the self-consistency cycle we still have to calculate the effective single-particle potential. Again, we rely on density functional theory and the local

density approximation, which in an approximate manner cast the full many-body problem into a single-particle self-consistent field problem. The potential is then represented as the sum of the external, Hartree and exchange-correlation potential [10, 11, 36, 41, 45]. The external potential is the Coulomb potential originating from the nuclei and possibly from external electromagnetic fields. In contrast, the Hartree potential comprises the classical contribution to the electron-electron Coulomb interaction. Finally, the non-classical contributions are covered by the exchange-correlation potential.

For practical calculations it is useful to first combine the electron density of the electrons as calculated in the previous section with the density of the nuclei, which is given by

$$\rho_{nuc}(\mathbf{r}) = - \sum_i \delta(\mathbf{r}_i) Z_i. \quad (2.4.1)$$

The classical potential due to the resulting total density then contains both the external and the Hartree potential. It can be written as

$$\begin{aligned} v_{es}(\mathbf{r}) &= 2 \int d^3 \mathbf{r}' \frac{\rho_{el}(\mathbf{r}')}{|\mathbf{r} - \mathbf{r}'|} - 2 \sum_{\mu i} \frac{Z_i}{|\mathbf{r} - \mathbf{R}_{\mu i}|} \\ &= 2 \sum_{\mu i} \int_{\Omega_i} d^3 \mathbf{r}'_{\mu i} \frac{\rho_{el}(\mathbf{r}'_{\mu i})}{|\mathbf{r}_{\mu i} - \mathbf{r}'_{\mu i}|} - 2 \sum_{\mu i} \frac{Z_i}{|\mathbf{r}_{\mu i}|}. \end{aligned} \quad (2.4.2)$$

The prefactor 2 entering here is due to our choice of atomic units, where it is identical to e^2 . It reflects the fact that so far we have calculated electron and nuclear densities rather than charge densities. Since the Coulomb potential requires a charge density an extra factor e has to be added.

Next we assume the position \mathbf{r} to lie in the atomic sphere centered at the site \mathbf{R}_{vj} . Using the identity [37, (3.70)]

$$\frac{1}{|\mathbf{r} - \mathbf{r}'|} = \sum_L \frac{4\pi}{2l+1} \frac{r_{<}^l}{r_{>}^{l+1}} Y_L^*(\hat{\mathbf{r}}) Y_L(\hat{\mathbf{r}'}), \quad (2.4.3)$$

which follows from (3.6.8) for $\kappa \rightarrow 0$, we transform (2.4.2) into the following expression

$$\begin{aligned} v_{es}(\mathbf{r})|_{|\mathbf{r}_{vj}| \leq S_j} &= 8\pi \frac{1}{r_{vj}} \int_0^{r_{vj}} dr'_{vj} r_{vj}'^2 \rho_{el}(r'_{vj}) + 8\pi \int_{r_{vj}}^{S_j} dr'_{vj} r_{vj}' \rho_{el}(r'_{vj}) \\ &\quad - 2 \frac{Z_i}{|\mathbf{r}_{vj}|} + 2 \sum_{\mu i} (1 - \delta_{\mu v} \delta_{ij}) \frac{Q_i - Z_i}{|\mathbf{r}_{\mu i}|}. \end{aligned} \quad (2.4.4)$$

It is based on the shape approximation, i.e. on the assumption of spherical symmetric electron densities confined to atomic spheres, which we used already in Sect. 2.3 for the electron density. In (2.4.4), we have furthermore separated all charges contained

in the sphere centered at the site \mathbf{R}_{vj} from those falling outside this sphere. In doing so, we have used the definition of point charges

$$Q_i := 4\pi \int_0^{S_i} dr'_{\mu i} r'^2_{\mu i} \rho_{el}(r'_{\mu i}) \quad (2.4.5)$$

as resulting from integrating all the electronic charge within an atomic sphere. This is motivated by the fact that, if viewed from outside a sphere, a spherical symmetric charge density within a sphere acts like a point charge located at its center. If combined with the nuclear charges these “electronic point charges” generate the Madelung potential, which is represented by the last term in (2.4.4). However, it is important to note that this treatment neglects the overlap of the atomic spheres, which is substantial especially in the atomic-sphere approximation. This leads to an error in the potential and, in particular, in the total energy to be calculated in Sect. 2.5. The error is rather small in closed packed solids, where the overlap can be minimized [30, 53, 67]. Yet, it is large enough to spoil the calculation of phonon frequencies and forces. It is the aim of a full-potential ASW method to overcome the shape approximation and to provide higher accuracy for the total energy and the potential.

Still, we can substantially simplify the Madelung term in (2.4.4) by consequently using the muffin-tin shape of the potential. Due to the spherical symmetry of the potential within the atomic spheres, which suppresses the angular degrees of freedom, the Madelung potential, e.g., in the sphere at site \mathbf{R}_{vj} , can in no way depend on the position \mathbf{r}_{vj} within that sphere. For that reason, the Madelung potential reduces to

$$v_{Mad,j} = 2 \sum_{\mu i} (1 - \delta_{0\mu} \delta_{ij}) \frac{Q_i - Z_i}{|\boldsymbol{\tau}_j - \boldsymbol{\tau}_i - \mathbf{R}_\mu|}, \quad (2.4.6)$$

which is just a constant shift of the potential within each atomic sphere.

The lattice sum entering (2.4.6) is closely related to the $\mathbf{k} = \mathbf{0}$ -Bloch-summed Hankel function discussed in Sect. 3.5. Using the asymptotic form of the barred Hankel function (3.1.45) and the relation (3.1.17) we write

$$\bar{h}_0^{(1)}(\kappa r) \stackrel{\kappa r \rightarrow 0}{\sim} \frac{1}{r} \quad (2.4.7)$$

and

$$H_{L\kappa}(\boldsymbol{\tau}_j - \boldsymbol{\tau}_i - \mathbf{R}_\mu)|_{l=0, \kappa \rightarrow 0} = \frac{1}{\sqrt{4\pi}} \frac{1}{|\boldsymbol{\tau}_j - \boldsymbol{\tau}_i - \mathbf{R}_\mu|}. \quad (2.4.8)$$

Comparing this to the definition (3.5.2) of the Bloch-summed Hankel envelope function we obtain for the Madelung potential (2.4.6) the result

$$\begin{aligned} v_{Mad,j} &= 2 \sum_{\mu i} (1 - \delta_{0\mu} \delta_{ij}) \sqrt{4\pi} H_{L\kappa}(\boldsymbol{\tau}_j - \boldsymbol{\tau}_i - \mathbf{R}_\mu) (Q_i - Z_i)|_{l=0, \kappa \rightarrow 0} \\ &= 2 \sum_i \sqrt{4\pi} D_{L\kappa}(\boldsymbol{\tau}_j - \boldsymbol{\tau}_i, \mathbf{0}) (Q_i - Z_i)|_{l=0, \kappa \rightarrow 0}. \end{aligned} \quad (2.4.9)$$

Note that those parts of the Bloch-summed Hankel function $D_{L\kappa}$, which do not depend on the vector $\boldsymbol{\tau}_j - \boldsymbol{\tau}_i$, cancel out due to charge neutrality of the unit cell,

$$\sum_i (Q_i - Z_i) \stackrel{!}{=} 0. \quad (2.4.10)$$

This holds especially for the term with $\mathbf{K}_n = \mathbf{0}$ in the reciprocal lattice sum of the function $D_{L\kappa}^{(1)}$, which is defined by (3.5.19). Since this term does not depend on the index j for $\mathbf{k} = \mathbf{0}$ the sum over all charges vanishes and the singular behavior for $\mathbf{K}_n = \mathbf{0}$ is avoided [22].

Having calculated the classical parts of the single-particle potential we turn to the exchange-correlation potential. As already mentioned, we use the local density approximation, which returns the exchange-correlation potential as a spin-dependent local function of the spin-dependent electronic densities [10, 11, 41, 42, 45, 77], and write

$$\begin{aligned} v_{xc,\sigma}(\mathbf{r}) &= v_{xc,\sigma}[\rho_{el,\sigma}(\mathbf{r}), \rho_{el,-\sigma}(\mathbf{r})] \\ &= \sum_i v_{xc,i\sigma}[\rho_{el,\sigma}(\mathbf{r}_i), \rho_{el,-\sigma}(\mathbf{r}_i)] \\ &= \sum_i v_{xc,i\sigma}(\mathbf{r}_i). \end{aligned} \quad (2.4.11)$$

In the past, several parametrizations for the density dependence of the exchange-correlation potential have been derived from different treatments of the homogeneous electron gas among them those proposed by Hedin and Lundqvist, von Barth and Hedin, Moruzzi, Williams and Janak, Vosko, Wilk and Nusair, and Perdew and Zunger [10, 12, 28, 34, 45, 54, 62, 75]. A complete overview of all these parametrizations was given by MacLaren et al. [49]. Alternatively, we may employ the generalized gradient approximation, for which parametrizations were given by Perdew and coworkers, Engel and Vosko, and Zhang and Yang [20, 48, 57–61, 79].

Combining (2.4.4), (2.4.9), and (2.4.11) we arrive at the following result for the effective single-particle potential

$$\begin{aligned} v_\sigma(\mathbf{r}) &= v_{es}(\mathbf{r}) + v_{xc,\sigma}(\mathbf{r}) \\ &= \sum_i [v_{es,i}(\mathbf{r}_i) + v_{xc,i\sigma}(\mathbf{r}_i) + v_{Mad,i}] \\ &= \sum_i v_\sigma(\mathbf{r}_i). \end{aligned} \quad (2.4.12)$$

Here

$$v_{es,i}(\mathbf{r}_i) = 8\pi \frac{1}{r_i} \int_0^{r_i} dr'_i r_i'^2 \rho_{el}(r'_i) + 8\pi \int_{r_i}^{S_i} dr'_i r_i' \rho_{el}(r'_i) - 2 \frac{Z_i}{|\mathbf{r}_i|} \quad (2.4.13)$$

is the electrostatic potential generated by all charges within the same sphere, which deviates from the expression (2.4.13) by the Madelung term representing the potential generated by all charges outside the respective sphere. Due to this separation of

intraatomic contributions from the outside charges the calculations are significantly simplified. In a last step, we have to specify the muffin-tin zero, which is usually set to the average of the potentials at the surfaces of the atomic spheres.

By now, we have closed the self-consistency cycle since the just derived potential can be inserted into Schrödinger's equations (2.1.14) and (2.1.21) this allowing for the calculation of new augmented Hankel and Bessel functions. Nevertheless, there is an additional bonus due to the previous separation of the Madlung potential, which induces only a constant potential shift in each atomic sphere. As a consequence, all the intraatomic problems are completely decoupled, and we are able to calculate the intraatomic potential according to (2.4.12) without taking the Madlung term into account. Having finished this step we do not directly pass the potential to the following band calculation but instead insert it into Schrödinger's equation to calculate new radial functions and a new electron density. This establishes an intraatomic self-consistency cycle, which allows for a self-consistently calculated potential within each atom before all these atomic potentials are combined for the following step of the band iteration. This might save a lot of computation time.

To be specific, we describe the sequence of intraatomic calculations in more detail. Following the flow diagram given in Fig. 2.3 we start out from the energies $E_{li\sigma}^{(\alpha)}$ and electron numbers $Q_{li\sigma}^{(\alpha)}$ as resulting from the momentum analysis of the partial densities of states. The energies are then transformed to the local energy scale by setting

$$\bar{E}_{li\sigma}^{(\alpha)} = E_{li\sigma}^{(\alpha)} + v_{MTZ} - v_{Mad,i}. \quad (2.4.14)$$

After this we solve the radial Schrödinger equation

$$\begin{aligned} & \left[-\frac{1}{r_i} \frac{\partial^2}{\partial r_i^2} r_i + \frac{l(l+1)}{r_i^2} + v_{es,i}(\mathbf{r}_i) + v_{xc,i\sigma}(\mathbf{r}_i) - v_{MTZ} - E_{li\sigma}^{(\alpha)} \right] R_{l\sigma}(\bar{E}_{li\sigma}^{(\alpha)}, r_i) \\ &= \left[-\frac{1}{r_i} \frac{\partial^2}{\partial r_i^2} r_i + \frac{l(l+1)}{r_i^2} + v_{es,i}(\mathbf{r}_i) + v_{xc,i\sigma}(\mathbf{r}_i) - v_{Mad,i} - \bar{E}_{li\sigma}^{(\alpha)} \right] \\ & \times R_{l\sigma}(\bar{E}_{li\sigma}^{(\alpha)}, r_i) = 0, \end{aligned} \quad (2.4.15)$$

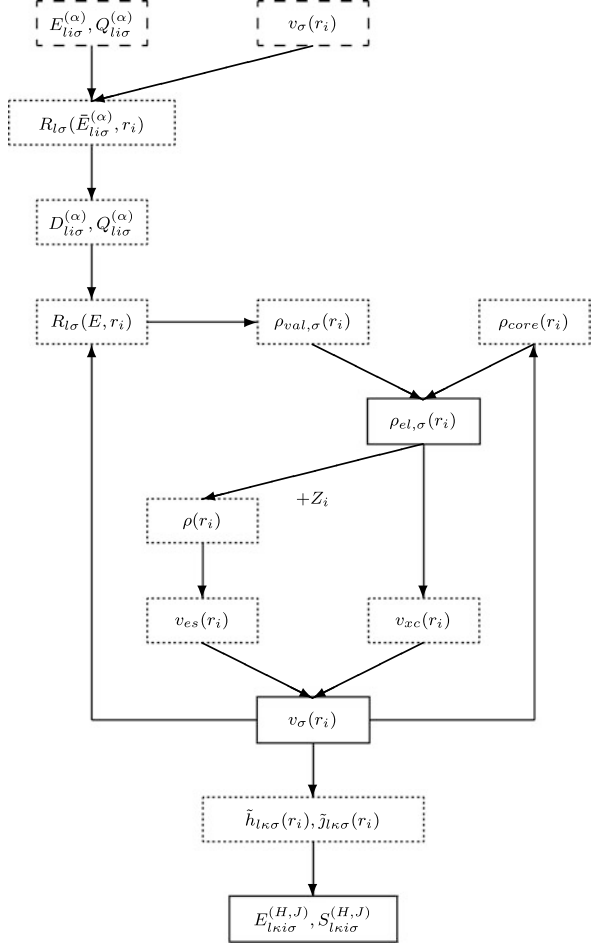
where $R_{l\sigma}(\bar{E}_{li\sigma}^{(\alpha)}, r_i)$ is a real and regular function normalized to

$$\int_0^{S_i} dr_i r_i^2 |R_{l\sigma}(\bar{E}_{li\sigma}^{(\alpha)}, r_i)|^2 = Q_{li\sigma}^{(\alpha)}. \quad (2.4.16)$$

From the solution of the radial equation (2.4.15) we then get the logarithmic derivatives at the sphere boundary

$$\begin{aligned} D_{li\sigma}^{(\alpha)}(\bar{E}_{li\sigma}^{(\alpha)}) &= \frac{\partial}{\partial r_i} (\ln R_{l\sigma}(\bar{E}_{li\sigma}^{(\alpha)}, r_i))_{r_i=S_i} \\ &= [R_{l\sigma}(\bar{E}_{li\sigma}^{(\alpha)}, S_i)]^{-1} \frac{\partial}{\partial r_i} R_{l\sigma}(\bar{E}_{li\sigma}^{(\alpha)}, r_i) \Big|_{r_i=S_i}. \end{aligned} \quad (2.4.17)$$

Fig. 2.3 Flow diagram of the intraatomic calculations of the standard ASW method. Input and output variables are highlighted by *dashed* and *solid* boxes, respectively



This way we arrive at a set of four new quantities per basis state, namely, the logarithmic derivatives $D_{liσ}^{(α)}$ and the electron numbers $Q_{liσ}^{(α)}$. As experience has shown, the logarithmic derivatives are superior to the energies $E_{liσ}^{(α)}$ as they allow for a more stable acceleration of the iteration process. In the course of the latter the logarithmic derivatives and the electron numbers of the actual iteration as well as previous ones are used to make a good guess for the following iteration. There exist many different methods for the acceleration of iteration processes in electronic structure calculations and a large number of original papers dealing with the issue [2, 9, 13–18, 29, 38, 39, 44, 64, 68, 71, 74]. For a recent overview see Ref. [24].

In addition to this rather numerical advantage of the logarithmic derivatives they allow for a better illustration of the interplay between intraatomic and band calculations. This has been used already in the concept of “renormalized atoms”. It corresponds to atomic calculations subject to boundary conditions, which reflect

the influence of the surrounding atoms [31, 35, 76, 78]. It is this concept, which, according to Williams, Kübler, and Gelatt, initiated the development of the ASW method [78].

Finally, with the logarithmic derivatives at hand we enter the intraatomic iteration cycle as sketched in Fig. 2.3. After self-consistency has been achieved, the muffin-tin potential is used in an additional step with the radial Schrödinger equations (2.1.14) and (2.1.21) as well as the boundary conditions (2.1.15) and (2.1.22) to evaluate the Hankel and Bessel energies $E_{lki\sigma}^{(H)}$ and $E_{lki\sigma}^{(J)}$ as well as the Hankel and Bessel integrals $S_{lki\sigma}^{(H)}$ and $S_{lki\sigma}^{(J)}$, which enter the subsequent band calculation.

2.5 Total Energy

In the previous sections we have learned about the major steps of the ASW method. This included the calculation of partial densities of states and partial occupation numbers, which already give a lot of information about the materials properties. However, in many cases the total energy is also of great interest. We just mention binding energies, bulk moduli, elastic constants or the stability of different magnetic structures. While some of these quantities are beyond the scope of the ASA and need a more accurate treatment as provided by a full-potential scheme, we will, nevertheless, in this last section of the present chapter sketch the evaluation of the total energy.

Within density functional theory, the total energy is given as the sum of the kinetic energy, the electrostatic energy arising from the classical part of the electron-electron interaction, and the exchange-correlation energy [10, 11, 19, 21, 28, 45, 56]. An additional contribution stems from the external potential, which, in the simplest case, is just the electrostatic potential generated by the nuclei. Finally, we have to add the energy due to the electrostatic interaction between the nuclei. We thus note

$$\begin{aligned}
 E_T &= E_T[\rho_{el,\uparrow}(\mathbf{r}), \rho_{el,\downarrow}(\mathbf{r})] \\
 &= T[\rho_{el,\uparrow}(\mathbf{r}), \rho_{el,\downarrow}(\mathbf{r})] + \sum_{\sigma} \int d^3\mathbf{r} v_{ext}(\mathbf{r}) \rho_{el,\sigma}(\mathbf{r}) \\
 &\quad + \frac{1}{N} \iint d^3\mathbf{r} d^3\mathbf{r}' \frac{\rho_{el}(\mathbf{r}) \rho_{el}(\mathbf{r}')}{|\mathbf{r} - \mathbf{r}'|} + E_{xc}[\rho_{el,\uparrow}(\mathbf{r}), \rho_{el,\downarrow}(\mathbf{r})] \\
 &\quad + \frac{1}{N} \sum_{\mu i} \sum_{\nu j} (1 - \delta_{\mu\nu} \delta_{ij}) \frac{Z_i Z_j}{|\mathbf{R}_{\nu j} - \mathbf{R}_{\mu i}|} \\
 &= T[\rho_{el,\uparrow}(\mathbf{r}), \rho_{el,\downarrow}(\mathbf{r})] + E_{es}[\rho_{el}(\mathbf{r})] + E_{xc}[\rho_{el,\uparrow}(\mathbf{r}), \rho_{el,\downarrow}(\mathbf{r})], \quad (2.5.1)
 \end{aligned}$$

where all integrations extend over the whole crystal unless otherwise indicated and N denotes the number of unit cells. In addition, we have used atomic units as defined in Sect. 1.2, i.e. $e^2 = 2$. Furthermore, we have in the last step combined all the contributions arising from the classical part of the Coulomb interaction into the total electrostatic energy. The three terms on the right-hand side are now subject to further inspection.

An expression for the kinetic energy grows out of the Kohn-Sham equations by multiplying them with the complex conjugate of the respective wave function, summing over all eigenstates and integrating over all space [19, 21, 28, 56]. From this we obtain

$$T[\rho_{el,\uparrow}(\mathbf{r}), \rho_{el,\downarrow}(\mathbf{r})] = \sum_{\mathbf{k}\sigma} E_{\sigma}(\mathbf{k})\Theta(E_F - E_{\sigma}(\mathbf{k})) + \sum_{nlmi\sigma} E_{nli\sigma} + v_{MTZ} \sum_i Q_i - \sum_{\sigma} \int d^3\mathbf{r} v_{\sigma}(\mathbf{r})\rho_{el,\sigma}(\mathbf{r}). \quad (2.5.2)$$

Here, the third term takes care of the fact that the single-particle energies were referred to the muffin-tin zero whereas the potential is not. The latter is given by

$$v_{\sigma}(\mathbf{r}) = v_{es}^{(el)}(\mathbf{r}) + v_{xc,\sigma}(\mathbf{r}) + v_{ext}(\mathbf{r}), \quad (2.5.3)$$

where

$$v_{es}^{(el)}(\mathbf{r}) = 2 \int d^3\mathbf{r}' \frac{\rho_{el}(\mathbf{r}')}{|\mathbf{r} - \mathbf{r}'|} \quad (2.5.4)$$

is the electrostatic potential generated by the electronic density. As well known, (2.5.2) can be used to write the total energy as the sum of all single-particle energies (valence and core) minus the so-called “double counting” terms. Eventually, we will also arrive at an expression of this kind. However, we point out that the effective potential entering the kinetic energy is the potential *making* the single-particle energies and, hence, the electron density, whereas the potential entering the electrostatic energy is the potential *made* by the density. These two potentials should be distinguished as long as full self-consistency has not yet been reached. Nevertheless, according to (2.5.3) the potential entering the kinetic energy also contains the external potential, which does not change during the iterations and thus cancels the corresponding term in (2.5.1) exactly. Combining (2.5.1) to (2.5.3) we thus note

$$\begin{aligned} E_T &= \sum_{\mathbf{k}\sigma} E_{\sigma}(\mathbf{k})\Theta(E_F - E_{\sigma}(\mathbf{k})) + \sum_{nlmi\sigma} E_{nli\sigma} + v_{MTZ} \sum_i Q_i \\ &\quad - \sum_{\sigma} \int d^3\mathbf{r} [v_{es}^{(el)}(\mathbf{r}) + v_{xc,\sigma}(\mathbf{r}) + v_{ext}(\mathbf{r})]\rho_{el,\sigma}(\mathbf{r}) \\ &\quad + \sum_{\sigma} \int d^3\mathbf{r} v_{ext}(\mathbf{r})\rho_{el,\sigma}(\mathbf{r}) \\ &\quad + \frac{1}{N} \iint d^3\mathbf{r} d^3\mathbf{r}' \frac{\rho_{el}(\mathbf{r})\rho_{el}(\mathbf{r}')}{|\mathbf{r} - \mathbf{r}'|} + E_{xc}[\rho_{el,\uparrow}(\mathbf{r}), \rho_{el,\downarrow}(\mathbf{r})] \\ &\quad + \frac{1}{N} \sum_{\mu i} \sum_{\nu j} (1 - \delta_{\mu\nu}\delta_{ij}) \frac{Z_i Z_j}{|\mathbf{R}_{\nu j} - \mathbf{R}_{\mu i}|} \\ &= \sum_{\mathbf{k}\sigma} E_{\sigma}(\mathbf{k})\Theta(E_F - E_{\sigma}(\mathbf{k})) + \sum_{nlmi\sigma} E_{nli\sigma} + v_{MTZ} \sum_i Q_i \\ &\quad - \sum_{\sigma} \int d^3\mathbf{r} [v_{es}^{(el,in)}(\mathbf{r}) + v_{xc,\sigma}(\mathbf{r})]\rho_{el,\sigma}(\mathbf{r}) \end{aligned}$$

$$\begin{aligned}
& + \frac{1}{2} \sum_{\sigma} \int d^3 \mathbf{r} v_{es}^{(el,out)}(\mathbf{r}) \rho_{el,\sigma}(\mathbf{r}) + E_{xc}[\rho_{el,\uparrow}(\mathbf{r}), \rho_{el,\downarrow}(\mathbf{r})] \\
& + \frac{1}{N} \sum_{\mu i} \sum_{\nu j} (1 - \delta_{\mu\nu} \delta_{ij}) \frac{Z_i Z_j}{|\mathbf{R}_{\nu j} - \mathbf{R}_{\mu i}|} \\
& = \sum_{\mathbf{k}\sigma} E_{\sigma}(\mathbf{k}) \Theta(E_F - E_{\sigma}(\mathbf{k})) + \sum_{nlmi\sigma} E_{nli\sigma} + v_{MTZ} \sum_i Q_i \\
& - \frac{1}{2} \sum_{\sigma} \int d^3 \mathbf{r} v_{es}^{(el)}(\mathbf{r}) \rho_{el,\sigma}(\mathbf{r}) + \frac{1}{N} \sum_{\mu i} \sum_{\nu j} (1 - \delta_{\mu\nu} \delta_{ij}) \frac{Z_i Z_j}{|\mathbf{R}_{\nu j} - \mathbf{R}_{\mu i}|} \\
& + E_{xc}[\rho_{el,\uparrow}(\mathbf{r}), \rho_{el,\downarrow}(\mathbf{r})] - \sum_{\sigma} \int d^3 \mathbf{r} v_{xc,\sigma}(\mathbf{r}) \rho_{el,\sigma}(\mathbf{r}), \tag{2.5.5}
\end{aligned}$$

where we have omitted the integrals over the external potential in the second step. While at that stage we still have distinguished the potentials $v_{es}^{(el,in)}(\mathbf{r})$ *making* the electronic density and $v_{es}^{(el,out)}(\mathbf{r})$ *made from* the electronic density, these potentials were combined in the third step leading to the representation of the total energy as the sum of single-particle energies minus the double counting terms.

In further evaluating the total energy we aim at a formulation, which allows for both a simple calculation and interpretation of the results. Such a formulation is indeed possible and consists of a sum of atomic contributions plus the Madelung energy, which includes a sum over pairs of atomic sites,

$$E_T = \sum_i E_{T,i} + E_{Mad}. \tag{2.5.6}$$

In order to derive this representation we start from the band energy contribution to the total energy, which is the first term on the right-hand side of (2.5.5). It may be simplified a lot with the help of the definition (2.3.15) of the partial densities of states as well as the alternative representation (2.3.17) arising from the moment analysis. We thus note

$$\begin{aligned}
\sum_{\mathbf{k}\sigma} E_{\sigma}(\mathbf{k}) \Theta(E_F - E_{\sigma}(\mathbf{k})) &= \sum_{\sigma} \int_{-\infty}^{E_F} dE \sum_{\mathbf{k}} E_{\sigma}(\mathbf{k}) \delta(E - E_{\sigma}(\mathbf{k})) \\
&= \sum_{\sigma} \int_{-\infty}^{E_F} dE E \rho_{\sigma}(E) \\
&= \sum_{li\sigma} \int_{-\infty}^{E_F} dE E \rho_{li\sigma}(E) \\
&= \sum_{li\sigma} \sum_{\alpha=1}^2 E_{li\sigma}^{(\alpha)} Q_{li\sigma}^{(\alpha)}. \tag{2.5.7}
\end{aligned}$$

Using (2.4.14) we can still split off the local Madelung potential. Defining an analogous energy shift for the core states by

$$\bar{E}_{nli\sigma} := E_{nli\sigma} + v_{MTZ} - v_{Mad,i} \tag{2.5.8}$$

we obtain

$$\begin{aligned}
& \sum_{\mathbf{k}\sigma} E_{\sigma}(\mathbf{k}) \Theta(E_F - E_{\sigma}(\mathbf{k})) + \sum_{nlmi\sigma} E_{nli\sigma} + v_{MTZ} \sum_i Q_i \\
&= \sum_{li\sigma} \left[\sum_{\alpha=1}^2 E_{li\sigma}^{(\alpha)} Q_{li\sigma}^{(\alpha)} + (2l+1) \sum_n E_{nli\sigma} \right] \\
&= \sum_{li\sigma} \left[\sum_{\alpha=1}^2 \bar{E}_{li\sigma}^{(\alpha)} Q_{li\sigma}^{(\alpha)} + (2l+1) \sum_n \bar{E}_{nli\sigma} \right] \\
&+ \sum_i v_{Mad,i} \left[\sum_{l\sigma} \sum_{\alpha=1}^2 Q_{li\sigma}^{(\alpha)} + 2 \sum_{nl} (2l+1) \right]. \tag{2.5.9}
\end{aligned}$$

The last square-bracket term on the right-hand side is the total electron number inside the atomic sphere at site \mathbf{r}_i , which we defined as Q_i in (2.4.5). In addition, we have from (2.3.19) and (2.3.20)

$$\sum_{l\sigma} \sum_{\alpha=1}^2 Q_{li\sigma}^{(\alpha)} = 4\pi \sum_{\sigma} \int_0^{S_i} \rho_{val,i\sigma}(r_i) \tag{2.5.10}$$

and

$$2 \sum_{n,l} (2l+1) = 4\pi \sum_{\sigma} \int_0^{S_i} \rho_{core,\sigma}(r_i). \tag{2.5.11}$$

Combining (2.5.7) to (2.5.9) we arrive at the following expression for the sum of the single-particle energies

$$\begin{aligned}
& \sum_{\mathbf{k}\sigma} E_{\sigma}(\mathbf{k}) \Theta(E_F - E_{\sigma}(\mathbf{k})) + \sum_{nlmi\sigma} E_{nli\sigma} + v_{MTZ} \sum_i Q_i \\
&= \sum_{li\sigma} \left[\sum_{\alpha=1}^2 \bar{E}_{li\sigma}^{(\alpha)} Q_{li\sigma}^{(\alpha)} + (2l+1) \sum_n \bar{E}_{nli\sigma} \right] + \sum_i v_{Mad,i} Q_i. \tag{2.5.12}
\end{aligned}$$

Next we turn to the electronic contribution to the electrostatic energy. Due to our previous choice of the ASA and the resulting neglect of the interstitial region the integrals over the whole crystal turn into sums of integrals over atomic spheres. However, as for the construction of the Hartree potential, the latter integrals can be replaced by point charges located at the sphere centers whenever the twofold integral extends over different spheres. We thus note

$$\begin{aligned}
& -\frac{1}{2} \sum_{\sigma} \int d^3\mathbf{r} v_{es}^{(el)}(\mathbf{r}) \rho_{el,\sigma}(\mathbf{r}) \\
&= -\frac{1}{N} \iint d^3\mathbf{r} d^3\mathbf{r}' \frac{\rho_{el}(\mathbf{r}) \rho_{el}(\mathbf{r}')}{|\mathbf{r} - \mathbf{r}'|} \\
&= -\frac{1}{N} \sum_{\mu\nu} \sum_{ij} \int_{\Omega_i} \int_{\Omega_j} d^3\mathbf{r}_{\mu i} d^3\mathbf{r}'_{\nu j} \frac{\rho_{el,i}(\mathbf{r}_i) \rho_{el,j}(\mathbf{r}'_j)}{|\mathbf{r}_{\mu i} - \mathbf{r}'_{\nu j}|}
\end{aligned}$$

$$\begin{aligned}
&= - \sum_i \int_{\Omega_i} \int_{\Omega_i} d^3\mathbf{r}_i d^3\mathbf{r}'_i \frac{\rho_{el,i}(\mathbf{r}_i) \rho_{el,i}(\mathbf{r}'_i)}{|\mathbf{r}_i - \mathbf{r}'_i|} \\
&\quad - \frac{1}{N} \sum_{\mu\nu} \sum_{ij} (1 - \delta_{\mu\nu} \delta_{ij}) \frac{Q_i Q_j}{|\mathbf{R}_{\mu i} - \mathbf{R}_{\nu j}|} \\
&=: - \frac{1}{2} \sum_i \int_{\Omega_i} d^3\mathbf{r}_i \bar{v}_{es,i}^{(el)}(\mathbf{r}_i) \rho_{el,i}(\mathbf{r}_i) \\
&\quad - \frac{1}{N} \sum_{\mu\nu} \sum_{ij} (1 - \delta_{\mu\nu} \delta_{ij}) \frac{Q_i Q_j}{|\mathbf{R}_{\mu i} - \mathbf{R}_{\nu j}|}, \tag{2.5.13}
\end{aligned}$$

where $\bar{v}_{es,i}^{(el)}(\mathbf{r}_i)$ denotes the electrostatic potential in the atomic sphere centered at τ_i and arising only from the electron density inside this sphere. In contrast, all intersphere interactions have been replaced by the electrostatic interaction of point charges located at the atomic sites. Of course, as already discussed in Sect. 2.4, this treatment means a severe approximation as soon as the atomic spheres overlap, which they do in the ASA. As a consequence of this and due to the complete neglect of the interstitial region, highly accurate total energies are beyond the ASA and can only be evaluated within a full-potential method.

Note that the electrostatic potential introduced in the last step of (2.5.13) is referred to the local potential zero. Defining the potential

$$v_{es,i}^{(el)}(\mathbf{r}) = \bar{v}_{es,i}^{(el)}(\mathbf{r}) + v_{Mad,i} \tag{2.5.14}$$

we may thus rewrite (2.5.13) as

$$\begin{aligned}
&- \frac{1}{2} \sum_{\sigma} \int d^3\mathbf{r} v_{es}^{(el)}(\mathbf{r}) \rho_{el,\sigma}(\mathbf{r}) \\
&= \frac{1}{2} \sum_i \int_{\Omega_i} d^3\mathbf{r}_i \bar{v}_{es,i}^{(el)}(\mathbf{r}_i) \rho_{el,i}(\mathbf{r}_i) \\
&\quad - \sum_i \int_{\Omega_i} d^3\mathbf{r}_i v_{es,i}^{(el)}(\mathbf{r}_i) \rho_{el,i}(\mathbf{r}_i) + \sum_i v_{Mad,i} \int_{\Omega_i} d^3\mathbf{r}_i \rho_{el,i}(\mathbf{r}_i) \\
&\quad - \frac{1}{N} \sum_{\mu\nu} \sum_{ij} (1 - \delta_{\mu\nu} \delta_{ij}) \frac{Q_i Q_j}{|\mathbf{R}_{\mu i} - \mathbf{R}_{\nu j}|} \\
&= \frac{1}{2} \sum_i \int_{\Omega_i} d^3\mathbf{r}_i \bar{v}_{es,i}^{(el)}(\mathbf{r}_i) \rho_{el,i}(\mathbf{r}_i) \\
&\quad - \sum_i \int_{\Omega_i} d^3\mathbf{r}_i v_{es,i}^{(el)}(\mathbf{r}_i) \rho_{el,i}(\mathbf{r}_i) + \sum_i v_{Mad,i} Q_i \\
&\quad - \frac{1}{N} \sum_{\mu\nu} \sum_{ij} (1 - \delta_{\mu\nu} \delta_{ij}) \frac{Q_i Q_j}{|\mathbf{R}_{\mu i} - \mathbf{R}_{\nu j}|}. \tag{2.5.15}
\end{aligned}$$

Here we have divided the intraatomic contributions into two integrals, where the potential is referred either to the local Madelung potential or else to the global potential zero. Combining (2.5.15) with the term comprising the interaction between the nuclei we arrive at the result

$$\begin{aligned}
& -\frac{1}{2} \sum_{\sigma} \int d^3 \mathbf{r} v_{es}^{(el)}(\mathbf{r}) \rho_{el,\sigma}(\mathbf{r}) + \frac{1}{N} \sum_{\mu i} \sum_{vj} (1 - \delta_{\mu v} \delta_{ij}) \frac{Z_i Z_j}{|\mathbf{R}_{vj} - \mathbf{R}_{\mu i}|} \\
& = \frac{1}{2} \sum_i \int_{\Omega_i} d^3 \mathbf{r}_i \bar{v}_{es,i}^{(el)}(\mathbf{r}_i) \rho_{el,i}(\mathbf{r}_i) - \sum_i \int_{\Omega_i} d^3 \mathbf{r}_i v_{es,i}^{(el)}(\mathbf{r}_i) \rho_{el,i}(\mathbf{r}_i) \\
& \quad - \frac{1}{N} \sum_{\mu v} \sum_{ij} (1 - \delta_{\mu v} \delta_{ij}) \frac{Q_i Q_j}{|\mathbf{R}_{\mu i} - \mathbf{R}_{vj}|} + \sum_i v_{Mad,i} Q_i \\
& \quad + \frac{1}{N} \sum_{\mu i} \sum_{vj} (1 - \delta_{\mu v} \delta_{ij}) \frac{Z_i Z_j}{|\mathbf{R}_{vj} - \mathbf{R}_{\mu i}|}. \tag{2.5.16}
\end{aligned}$$

The last three terms can be combined into the Madelung energy, which, using (2.4.6), we rewrite as

$$\begin{aligned}
E_{Mad} & = -\frac{1}{N} \sum_{\mu v} \sum_{ij} (1 - \delta_{\mu v} \delta_{ij}) \frac{Q_i Q_j}{|\mathbf{R}_{\mu i} - \mathbf{R}_{vj}|} + \sum_i v_{Mad,i} Q_i \\
& \quad + \frac{1}{N} \sum_{\mu i} \sum_{vj} (1 - \delta_{\mu v} \delta_{ij}) \frac{Z_i Z_j}{|\mathbf{R}_{vj} - \mathbf{R}_{\mu i}|} \\
& = \sum_{\mu} \sum_{ij} (1 - \delta_{\mu 0} \delta_{ij}) \frac{[Z_i Z_j - Q_i Q_j + Q_i (Q_j - Z_j) + Q_j (Q_i - Z_i)]}{|\boldsymbol{\tau}_j - \boldsymbol{\tau}_i - \mathbf{R}_{\mu}|} \\
& = \sum_{\mu} \sum_{ij} (1 - \delta_{\mu 0} \delta_{ij}) \frac{(Q_i - Z_i)(Q_j - Z_j)}{|\boldsymbol{\tau}_j - \boldsymbol{\tau}_i - \mathbf{R}_{\mu}|} \\
& = \frac{1}{2} \sum_i v_{Mad,i} (Q_i - Z_i). \tag{2.5.17}
\end{aligned}$$

As a consequence, we obtain for the sum of all electrostatic contributions the result

$$\begin{aligned}
& -\frac{1}{2} \sum_{\sigma} \int d^3 \mathbf{r} v_{es}^{(el)}(\mathbf{r}) \rho_{el,\sigma}(\mathbf{r}) + \frac{1}{N} \sum_{\mu i} \sum_{vj} (1 - \delta_{\mu v} \delta_{ij}) \frac{Z_i Z_j}{|\mathbf{R}_{vj} - \mathbf{R}_{\mu i}|} \\
& = \frac{1}{2} \sum_i \int_{\Omega_i} d^3 \mathbf{r}_i \bar{v}_{es,i}^{(el)}(\mathbf{r}_i) \rho_{el,i}(\mathbf{r}_i) - \sum_i \int_{\Omega_i} d^3 \mathbf{r}_i v_{es,i}^{(el)}(\mathbf{r}_i) \rho_{el,i}(\mathbf{r}_i) + E_{Mad} \\
& = -\frac{1}{2} \sum_i \int_{\Omega_i} d^3 \mathbf{r}_i \bar{v}_{es,i}^{(el)}(\mathbf{r}_i) \rho_{el,i}(\mathbf{r}_i) - \sum_i v_{Mad,i} Q_i + E_{Mad}. \tag{2.5.18}
\end{aligned}$$

Finally, the exchange-correlation energy is evaluated using the local density approximation [19, 21, 28, 56]

$$E_{xc,\sigma}[\rho_{el,\sigma}(\mathbf{r}), \rho_{el,-\sigma}(\mathbf{r})] = \frac{1}{N} \int d^3 \mathbf{r} \varepsilon_{xc,\sigma}[\rho_{el,\sigma}(\mathbf{r}), \rho_{el,-\sigma}(\mathbf{r})] \rho_{el,\sigma}(\mathbf{r}), \tag{2.5.19}$$

according to which the function $\varepsilon_{xc,\sigma}$ is a local function of the spin-dependent densities. In complete analogy to (2.4.11) we write

$$\begin{aligned}\varepsilon_{xc,\sigma}(\mathbf{r}) &= \varepsilon_{xc,\sigma}[\rho_{el,\sigma}(\mathbf{r}), \rho_{el,-\sigma}(\mathbf{r})] \\ &= \sum_i \varepsilon_{xc,i\sigma}[\rho_{el,\sigma}(\mathbf{r}_i), \rho_{el,-\sigma}(\mathbf{r}_i)] \\ &= \sum_i \varepsilon_{xc,i\sigma}(\mathbf{r}_i)\end{aligned}\quad (2.5.20)$$

again using one of the parametrizations mentioned in Sect. 2.4. With the local density approximation at hand the terms in the respective last lines of (2.5.5) can be written as

$$\begin{aligned}E_{xc,\sigma}[\rho_{el,\sigma}(\mathbf{r}), \rho_{el,-\sigma}(\mathbf{r})] &- \frac{1}{N} \int d^3\mathbf{r} v_{xc,\sigma}(\mathbf{r}) \rho_{el,\sigma}(\mathbf{r}) \\ &= \sum_i \int_{\Omega_i} d^3\mathbf{r}_i [\varepsilon_{xc,i\sigma}(\mathbf{r}_i) - v_{xc,i\sigma}(\mathbf{r}_i)] \rho_{el,i\sigma}(\mathbf{r}_i).\end{aligned}\quad (2.5.21)$$

Inserting the intermediate results (2.5.12), (2.5.18), and (2.5.21) into the initial formula (2.5.5) we arrive at two alternative final expressions for the total energy

$$\begin{aligned}E_T &= \sum_{li\sigma} \left[\sum_{\alpha=1}^2 \bar{E}_{li\sigma}^{(\alpha)} Q_{li\sigma}^{(\alpha)} + (2l+1) \sum_n \bar{E}_{nli\sigma} \right] \\ &\quad - \frac{1}{2} \sum_i \int_{\Omega_i} d^3\mathbf{r}_i \bar{v}_{es,i}^{(el)}(\mathbf{r}_i) \rho_{el,i}(\mathbf{r}_i) + E_{Mad} \\ &\quad + \sum_{i\sigma} \int_{\Omega_i} d^3\mathbf{r}_i [\varepsilon_{xc,i\sigma}(\mathbf{r}_i) - v_{xc,i\sigma}(\mathbf{r}_i)] \rho_{el,i\sigma}(\mathbf{r}_i) \\ &= \sum_{li\sigma} \left[\sum_{\alpha=1}^2 E_{li\sigma}^{(\alpha)} Q_{li\sigma}^{(\alpha)} + (2l+1) \sum_n E_{nli\sigma} \right] + v_{MTZ} \sum_i Q_i \\ &\quad + \frac{1}{2} \sum_i \int_{\Omega_i} d^3\mathbf{r}_i \bar{v}_{es,i}^{(el)}(\mathbf{r}_i) \rho_{el,i}(\mathbf{r}_i) - \sum_i \int_{\Omega_i} d^3\mathbf{r}_i v_{es,i}^{(el)}(\mathbf{r}_i) \rho_{el,i}(\mathbf{r}_i) + E_{Mad} \\ &\quad + \sum_{i\sigma} \int_{\Omega_i} d^3\mathbf{r}_i [\varepsilon_{xc,i\sigma}(\mathbf{r}_i) - v_{xc,i\sigma}(\mathbf{r}_i)] \rho_{el,i\sigma}(\mathbf{r}_i) \\ &= \sum_{li\sigma} \left[\sum_{\alpha=1}^2 E_{li\sigma}^{(\alpha)} Q_{li\sigma}^{(\alpha)} + (2l+1) \sum_n E_{nli\sigma} \right] + v_{MTZ} \sum_i Q_i \\ &\quad - \sum_{i\sigma} \int_{\Omega_i} d^3\mathbf{r}_i [v_{es,i}^{(el)}(\mathbf{r}_i) + v_{xc,i\sigma}(\mathbf{r}_i)] \rho_{el,i\sigma}(\mathbf{r}_i) \\ &\quad + \frac{1}{2} \sum_{i\sigma} \int_{\Omega_i} d^3\mathbf{r}_i \bar{v}_{es,i}^{(el)}(\mathbf{r}_i) \rho_{el,i\sigma}(\mathbf{r}_i) + \sum_{i\sigma} \int_{\Omega_i} d^3\mathbf{r}_i \varepsilon_{xc,i\sigma}(\mathbf{r}_i) \rho_{el,i\sigma}(\mathbf{r}_i) \\ &\quad + E_{Mad},\end{aligned}\quad (2.5.22)$$

where, in the last step, we have explicitly noted the double counting terms. From (2.5.22) the separation into a single and a double sum over atomic sites as already outlined in (2.5.6) is obvious. The atomic contributions are explicitly given by

$$\begin{aligned}
 E_{T,i} &= \sum_{l\sigma} \left[\sum_{\alpha=1}^2 \bar{E}_{li\sigma}^{(\alpha)} Q_{li\sigma}^{(\alpha)} + (2l+1) \sum_n \bar{E}_{nli\sigma} \right] \\
 &\quad - \frac{1}{2} \int_{\Omega_i} d^3\mathbf{r}_i \bar{v}_{es,i}^{(el)}(\mathbf{r}_i) \rho_{el,i}(\mathbf{r}_i) \\
 &\quad + \sum_{\sigma} \int_{\Omega_i} d^3\mathbf{r}_i [\varepsilon_{xc,i\sigma}(\mathbf{r}_i) - v_{xc,i\sigma}(\mathbf{r}_i)] \rho_{el,i\sigma}(\mathbf{r}_i) \\
 &= \sum_{l\sigma} \left[\sum_{\alpha=1}^2 E_{li\sigma}^{(\alpha)} Q_{li\sigma}^{(\alpha)} + (2l+1) \sum_n E_{nli\sigma} \right] + v_{MTZ} Q_i \\
 &\quad + \frac{1}{2} \int_{\Omega_i} d^3\mathbf{r}_i \bar{v}_{es,i}^{(el)}(\mathbf{r}_i) \rho_{el,i}(\mathbf{r}_i) - \int_{\Omega_i} d^3\mathbf{r}_i v_{es,i}^{(el)}(\mathbf{r}_i) \rho_{el,i}(\mathbf{r}_i) \\
 &\quad + \sum_{\sigma} \int_{\Omega_i} d^3\mathbf{r}_i [\varepsilon_{xc,i\sigma}(\mathbf{r}_i) - v_{xc,i\sigma}(\mathbf{r}_i)] \rho_{el,i\sigma}(\mathbf{r}_i) \\
 &= \sum_{l\sigma} \left[\sum_{\alpha=1}^2 E_{li\sigma}^{(\alpha)} Q_{li\sigma}^{(\alpha)} + (2l+1) \sum_n E_{nli\sigma} \right] + v_{MTZ} Q_i \\
 &\quad - \sum_{\sigma} \int_{\Omega_i} d^3\mathbf{r}_i [v_{es,i}^{(el)}(\mathbf{r}_i) + v_{xc,i\sigma}(\mathbf{r}_i)] \rho_{el,i\sigma}(\mathbf{r}_i) \\
 &\quad + \frac{1}{2} \sum_{\sigma} \int_{\Omega_i} d^3\mathbf{r}_i \bar{v}_{es,i}^{(el)}(\mathbf{r}_i) \rho_{el,i\sigma}(\mathbf{r}_i) + \sum_{\sigma} \int_{\Omega_i} d^3\mathbf{r}_i \varepsilon_{xc,i\sigma}(\mathbf{r}_i) \rho_{el,i\sigma}(\mathbf{r}_i)
 \end{aligned} \tag{2.5.23}$$

and the Madelung energy follows from (2.5.17).

References

1. M. Abramowitz, I.A. Stegun, *Handbook of Mathematical Functions* (Dover, New York, 1972)
2. H. Akai, P.H. Dederichs, J. Phys. C **18**, 2455 (1985)
3. O.K. Andersen, Comments on the KKR-wavefunction; Extension of the spherical wave expansion beyond the muffin-tins, in *Computational Methods in Band Theory*, ed. by P.M. Marcus, J.F. Janak, A.R. Williams (Plenum Press, New York, 1971), pp. 178–182
4. O.K. Andersen, Solid State Commun. **13**, 133 (1973)
5. O.K. Andersen, Phys. Rev. B **12**, 3060 (1975)
6. O.K. Andersen, Linear methods in band theory, in *The Electronic Structure of Complex Systems*, ed. by P. Phariseau, W. Temmerman (Plenum Press, New York, 1984), pp. 11–66
7. O.K. Andersen, Muffin-tin orbital theory, in *Methods on Electronic Structure Calculations*. Lecture Notes from the ICTP Workshop (International Center for Theoretical Physics, Trieste, 1992)

8. O.K. Andersen, O. Jepsen, D. Glötzel, Canonical description of the band structures of metals, in *Highlights of Condensed-Matter Theory*, ed. by F. Bassani, F. Fumi, M.P. Tosi. Proceedings of the International School of Physics "Enrico Fermi", Course LXXXIX (North-Holland, Amsterdam, 1985), pp. 59–176
9. D.G. Anderson, J. Assoc. Comput. Mach. **12**, 547 (1965)
10. U. von Barth, Density functional theory for solids, in *The Electronic Structure of Complex Systems*, ed. by P. Phariseau, W. Temmerman (Plenum Press, New York, 1984), pp. 67–140
11. U. von Barth, An overview of density functional theory, in *Many-Body Phenomena at Surfaces*, ed. by D. Langreth, H. Suhl (Academic Press, Orlando, 1984), pp. 3–50
12. U. von Barth, L. Hedin, J. Phys. C **5**, 1629 (1972)
13. P. Bendt, A. Zunger, Phys. Rev. B **26**, 3114 (1982)
14. S. Blügel, First principles calculations of the electronic structure of magnetic overlayers on transition metal surfaces, PhD thesis, Rheinisch-Westfälische Technische Hochschule Aachen, 1987
15. C.G. Broyden, Math. Comput. **19**, 577 (1965)
16. C.G. Broyden, Math. Comput. **21**, 368 (1966)
17. P.H. Dederichs, R. Zeller, Phys. Rev. B **28**, 5462 (1983)
18. J.E. Dennis Jr., J.J. Moré, SIAM Review **19**, 46 (1977)
19. R.M. Dreizler, E.K.U. Gross, *Density Functional Theory* (Springer, Berlin, 1990)
20. E. Engel, S.H. Vosko, Phys. Rev. B **47**, 13164 (1993)
21. H. Eschrig, *The Fundamentals of Density Functional Theory* (Edition am Gutenbergplatz, Leipzig, 2003)
22. P.P. Ewald, Ann. Phys. **64**, 253 (1921)
23. V. Eyert, Entwicklung und Implementation eines Full-Potential-ASW-Verfahrens, PhD thesis, Technische Hochschule Darmstadt, 1991
24. V. Eyert, J. Comput. Phys. **124**, 271 (1996)
25. V. Eyert, Electronic structure calculations for crystalline materials, in *Density Functional Methods: Applications in Chemistry and Materials Science*, ed. by M. Springborg (Wiley, Chichester, 1997), pp. 233–304
26. V. Eyert, Octahedral deformations and metal-insulator transition in transition metal chalcogenides, Habilitation thesis, University of Augsburg, 1998
27. V. Eyert, Int. J. Quantum Chem. **77**, 1007 (2000)
28. V. Eyert, *Electronic Structure of Crystalline Materials*, 2nd edn. (University of Augsburg, Augsburg, 2005)
29. L.G. Ferreira, J. Comput. Phys. **36**, 198 (1980)
30. E.R. Fuller, E.R. Naimon, Phys. Rev. B **6**, 3609 (1972)
31. C.D. Gelatt Jr., H. Ehrenreich, R.E. Watson, Phys. Rev. B **15**, 1613 (1977)
32. D. Hackenbracht, Berechnete elektronische und thermomechanische Eigenschaften einiger La-In und Al-Ni-Verbindungen, Diploma thesis, Ruhr-Universität Bochum, 1979
33. F.S. Ham, B. Segall, Phys. Rev. **124**, 1786 (1961)
34. L. Hedin, B.I. Lundqvist, J. Phys. C **4**, 2064 (1971)
35. L. Hodges, R.E. Watson, H. Ehrenreich, Phys. Rev. B **5**, 3953 (1972)
36. P. Hohenberg, W. Kohn, Phys. Rev. B **136**, 864 (1964)
37. J.D. Jackson, *Classical Electrodynamics* (Wiley, New York, 1975)
38. D.D. Johnson, Phys. Rev. B **38**, 12807 (1988)
39. G.P. Kerker, Phys. Rev. B **23**, 3082 (1981)
40. W. Kohn, N. Rostoker, Phys. Rev. **94**, 1111 (1954)
41. W. Kohn, L.J. Sham, Phys. Rev. A **140**, 1133 (1965)
42. W. Kohn, P. Vashishta, General density functional theory, in *Theory of the Inhomogeneous Electron Gas*, ed. by S. Lundqvist, N.H. March (Plenum Press, New York, 1983), pp. 79–147
43. J. Korringa, Physica **13**, 392 (1947)
44. G. Kresse, J. Furthmüller, Phys. Rev. B **54**, 11169 (1996)
45. J. Kübler, V. Eyert, Electronic structure calculations, in *Electronic and Magnetic Properties of Metals and Ceramics*, ed. by K.H.J. Buschow (VCH Verlagsgesellschaft, Weinheim, 1992),

- pp. 1–145; vol. 3A of *Materials Science and Technology*, ed. by R.W. Cahn, P. Haasen, E.J. Kramer (VCH Verlagsgesellschaft, Weinheim, 1991–1996)
46. J. Kübler, K.-H. Höck, J. Sticht, A.R. Williams, *J. Phys. F* **18**, 469 (1988)
 47. J. Kübler, K.-H. Höck, J. Sticht, A.R. Williams, *J. Appl. Phys.* **63**, 3482 (1988)
 48. M. Levy, J.P. Perdew, *Phys. Rev. B* **48**, 11638 (1993)
 49. J.M. MacLaren, D.P. Clougherty, M.E. McHenry, M.M. Donovan, *Comput. Phys. Commun.* **66**, 383 (1991)
 50. P.M. Marcus, J.F. Janak, A.R. Williams, *Computational Methods in Band Theory* (Plenum Press, New York, 1971)
 51. S.F. Matar, *Progr. Solid State Chem.* **31**, 239 (2003)
 52. A. Messiah, *Quantum Mechanics*, vol. 1 (North Holland, Amsterdam, 1976)
 53. M.S. Methfessel, Zur Berechnung der Lösungswärme von Metallhydriden, Diploma thesis, Ruhr-Universität Bochum, 1980
 54. V.L. Moruzzi, J.F. Janak, A.R. Williams, *Calculated Electronic Properties of Metals* (Pergamon Press, New York, 1978)
 55. W. Nolting, *Grundkurs: Theoretische Physik*, vol. 5, part 1: Quantenmechanik – Grundlagen (Springer, Berlin, 2004)
 56. R.G. Parr, W. Yang, *Density Functional Theory of Atoms and Molecules* (Oxford University Press, Oxford, 1989)
 57. J.P. Perdew, Unified theory of exchange and correlation beyond the local density approximation, in *Electronic Structure of Solids '91*, ed. by P. Ziesche, H. Eschrig (Akademie Verlag, Berlin, 1991), pp. 11–20
 58. J.P. Perdew, K. Burke, M. Ernzerhof, *Phys. Rev. Lett.* **77**, 3865 (1996)
 59. J.P. Perdew, K. Burke, Y. Wang, *Phys. Rev. B* **54**, 16533 (1996)
 60. J.P. Perdew, J.A. Chevary, S.H. Vosko, K.A. Jackson, M.R. Pederson, D.J. Singh, C. Fiolhais, *Phys. Rev. B* **46**, 6671 (1992)
 61. J.P. Perdew, Y. Wang, *Phys. Rev. B* **33**, 8800 (1986)
 62. J.P. Perdew, A. Zunger, *Phys. Rev. B* **23**, 5048 (1981)
 63. W.H. Press, B.P. Flannery, S.A. Teukolsky, W.T. Vetterling, *Numerical Recipes—The Art of Scientific Computing* (Cambridge University Press, Cambridge, 1989)
 64. P. Pulay, *Chem. Phys. Lett.* **73**, 393 (1980)
 65. L.M. Sandratskii, *Adv. Phys.* **47**, 91 (1998)
 66. B. Segall, F.S. Ham, in *Methods in Computational Physics*, ed. by B. Alder, S. Fernbach, M. Rotenberg (Academic Press, New York, 1968), pp. 251–293
 67. C.A. Sholl, *Proc. Phys. Soc.* **92**, 434 (1967)
 68. D. Singh, H. Krakauer, C.S. Wang, *Phys. Rev. B* **34**, 8391 (1986)
 69. H.L. Skriver, *The LMTO Method* (Springer, Berlin, 1984)
 70. J.C. Slater, *Phys. Rev.* **51**, 846 (1937)
 71. G.P. Srivastava, *J. Phys. A* **17**, L317 (1984)
 72. J. Sticht, K.-H. Höck, J. Kübler, *J. Phys.: Cond. Matt.* **1**, 8155 (1989)
 73. J. Sticht, Bandstrukturechnung für Schwere-Fermionen-Systeme, PhD thesis, Technische Hochschule Darmstadt, 1989
 74. D. Vanderbilt, S.G. Louie, *Phys. Rev. B* **30**, 6118 (1984)
 75. S.H. Vosko, L. Wilk, M. Nusair, *Can. J. Phys.* **58**, 1200 (1980)
 76. R.E. Watson, H. Ehrenreich, L. Hodges, *Phys. Rev. Lett.* **15**, 829 (1970)
 77. A.R. Williams, U. von Barth, Applications of density functional theory to atoms, molecules and solids, in *Theory of the Inhomogeneous Electron Gas*, ed. by S. Lundqvist, N.H. March (Plenum Press, New York, 1983), pp. 189–307
 78. A.R. Williams, J. Kübler, C.D. Gelatt Jr., *Phys. Rev. B* **19**, 6094 (1979)
 79. Y. Zhang, W. Yang, *Phys. Rev. Lett.* **80**, 890 (1998)

The Augmented Spherical Wave Method

A Comprehensive Treatment

Eyert, V.

2013, XV, 379 p., Softcover

ISBN: 978-3-642-25863-3